BIODIVERSITAS
Volume 26, Number 4, April 2025
Pages: 1590-1606

ISSN: 1412-033X
E-ISSN: 2085-4722
DOI: 10.13057/biodiv/d260411

Harnessing the metabolites from the marine sponge *Melophlus sarasinorum* for the discovery of eco-friendly antifoulants

WALTER BALANSA[1,♥], RIYANTI[2], MARIA A. PATRAS[3,7], KIRSTEN H. BALANSA[4], NOVRIYANDI HANIF[5], FRETS J. RIEUWPASSA[1], MARGARET HILL[6], TILL F. SCHÄBERLE[3,7]

[1]Department of Fishery and Maritime Technology, Politeknik Negeri Nusa Utara. Jl. Kesehatan No. 1, Kepulauan Sangihe 95812, North Sulawesi, Indonesia. Tel.: +62-432-24745, ♥email: walter.balansa@fulbrightmail.org
[2]Faculty of Fisheries and Marine Science, Universitas Jenderal Soedirman. Jl. Dr. Soeparno, Banyumas 53122, Central Java, Indonesia
[3]Fraunhofer Institute for Molecular Biology and Applied Ecology, Branch for Bioresources. Ohlebergsweg 12, Giessen 35392, Germany
[4]Department of Informatics Engineering, Faculty of Engineering, Universitas Sam Ratulangi. Jl. Unsrat Campus, Manado 95115, North Sulawesi, Indonesia
[5]Department of Chemistry, Faculty of Mathematics and Natural Sciences, Institut Pertanian Bogor. Jl. Meranti, Kampus IPB Dramaga, Bogor 16680, West Java, Indonesia
[6]Department of Biomedical and Pharmaceutical Sciences, College of Pharmacy, University of Rhode Island. 7 Greenhouse Rd., Kingston, RI 02881, USA
[7]Institute for Insect Biotechnology, Justus-Liebig-University of Giessen. Heinrich-Buff-Ring 26-32, 35392 Gießen, Germany

Manuscript received: 16 July 2024. Revision accepted: 27 March 2025.

Abstract. *Balansa W, Riyanti, Patras MA, Balansa KH, Hanif N, Rieuwpassa FJ, Hill M, Schäberle TF. 2025. Harnessing the metabolites from the marine sponge* Melophlus sarasinorum *for the discovery of eco-friendly antifoulants. Biodiversitas 26: 1590-1606.* Marine biofouling remains an unresolved issue in both the maritime industry and the marine environment, demanding the discovery of new eco-friendly antifoulants. This study aimed to evaluate the antifouling potential of the marine sponge, *Melophlus sarasinorum* (Thiele, 1899), through metabolomic, computational, and field studies. Seven compounds were dereplicated as sarasinosides A1-A3, D, L, M, and M2 (**1-7**) from extracts of *M. sarasinorum* from Kawaluso and Mahumu Islands. Molecular docking showed robust binding affinities for **1-7** (–8.2 to –9.6 kcal/mol), rivaling acetylcholinesterase (AChE) inhibitors, synoxazolidinones A (**8**) and C (**9**), commercial antifoulants medetomidine/selektope® (**12**) and econea® (**13**) (–9.2, –9.3, –9.5, –9.3 kcal/mol, respectively) as well as the antifouling agents, seanin_211 (**10**) (–8.9 kcal/mol) and irgarol_1505 (**11**) (–5.5, –6.5 kcal/mol, respectively). The strong binding affinities of **1-7** suggest possible new allosteric interactions with AChE. The ANOVA test revealed a significant difference in biofouling growth ($p<0.05$) between nets pre-treated with 1:1, 1:2, or 1:3 sponge powder/epoxy mixture compared to other treatments, as confirmed by a post-hoc Duncan test. Notably, toxicity studies with EPI Suite™ indicated that 1-7 had more eco-friendly toxicological parameters (i.e., low Log Kow, Log Koc, Biotransformation Half-life, and water solubility) compared to AChE inhibitors and commercial antifouling agents ($p<0.05$). Our results demonstrate the antifouling activity of sarasinosides (**1-7**), providing insight into the design of novel, eco-friendly antifoulants that warrant further investigation into their mode of action and optimization.

Keywords: Antifouling, eco-friendly, *Melophlus*, metabolomics, sarasinoside

INTRODUCTION

Biofouling remains a significant issue for the marine environment and maritime industries, with far-reaching ecological consequences. In the shipping industry, this leads to material corrosion, engine wear, and increased fuel consumption, resulting in higher operational costs and higher greenhouse gas emissions (Farkas et al. 2021; Song et al. 2021). The cost of biofouling is estimated to be a substantial USD 25 billion per year by 2100 (Olick 2023). With the continuous expansion of global shipping, it is anticipated that this sector will account for 10% of global greenhouse gas emissions by 2050 (Ayesu 2023). Furthermore, fouled ships can also act as vectors, capable of introducing invasive species to new marine environments and having negative ecological and economic consequences (Georgiades et al. 2021; Yousef 2023). Invasive species frequently compete with native species for resources, disrupt existing food webs, and induce significant shifts in ecosystem dynamics (Byers et al. 2023), endangering local biodiversity and ecological stability (Costanzo et al. 2021). This also increases the economic burden, estimated to be a staggering 345 billion USD annually (Cuthbert et al. 2021; Ross et al. 2024).

Similarly, in aquaculture, biofouling organisms have various negative effects, demanding regular and costly maintenance (Hadžić et al. 2022). Biofouling organisms obstruct water flow, lead to stagnant conditions, and reduce oxygen levels, making them critical indicators of disease outbreaks (Bannister et al. 2019). These effects include direct harm from stinging organisms, pathogen harboring and proliferation (e.g., vibriosis in cod), and disease transmission via vectors or intermediate hosts (e.g., blood flukes in tuna). Collectively, they damage existing infrastructure and increase operating costs, contributing to 5-10% of production-related expenses or equivalent to 1.5 to 3 billion USD per year (Bannister et al. 2019). The substantial financial burden makes the development of new and environmentally benign antifoulants a high priority (Dobretsov and Rittschof 2023).

Despite its effectiveness, tributyltin (TBT) was banned in 2003 due to its toxicity to marine life, the environment,

and human health (Selim et al. 2017). This ban has spurred the search for environmentally benign alternatives (Qian et al. 2015; Gomez-Banderas 2022). Research has focused on natural sources, including marine organisms (invertebrates, algae, and symbiotic microorganisms) (Qian et al. 2015; Bannister et al. 2019; Pinteus et al. 2021; Gomez-Banderas 2022) and terrestrial plants (Chen et al. 2021, 2023). These investigations have highlighted terpenoids, alkaloids, polyphenols, as promising antifoulants (Qian et al. 2015; Bannister et al. 2019; Chen et al. 2021, 2023). Current research also focuses on developing polymeric coatings with tailored antifouling properties, including: (i) Urushiol-based Benzoxazine Copper Polymer (UBCP) (Chen et al. 2021); (ii) UBCP/Polymerized Tung Oil (PTO) (Chen et al. 2023); (iii) composite coatings with in situ-generated silver nanoparticles for balanced antifouling efficacy and environmental compatibility (Chen et al. 2024a); and (iv) polybenzoxazine coatings with modulated surface energy and modulus (Chen et al. 2024b). Despite promising in vitro results, the ecological relevance of these novel antifoulants necessitates comprehensive field studies, and previously claimed "eco-friendly" agents require robust toxicity assessments (Quémener et al. 2022).

This study investigates the antifouling potential of *Melophlus sarasinorum* (Thiele, 1899) from the Sangihe Islands, Indonesia, employing a multidisciplinary approach. Metabolomics has significantly contributed to the elucidation of marine natural products, enabling rapid dereplication (Riyanti et al. 2020a). Molecular docking and in silico analyses have become indispensable components of the modern drug discovery process (Roney and Mohd Aluwi 2024) and in the development of antifouling agents (Arabshahi et al. 2021; Gaudêncio and Pereira 2022). Acetylcholinesterase (AChE) plays a key role in the settlement of both microfouling and macrofouling organisms. Its inhibition prevents the settlement of the tunicate *Ciona savignyi* (Herdman, 1882) (Arabshahi et al. 2021), mussel *Mytilus galloprovincialis* (Lamarck, 1819) larvae (Almeida et al. 2020), and several other biofouling bacteria (Arabshahi et al. 2021). This makes AChE, previously known as an Alzheimer's disease target (Marucci et al. 2021), an emerging antifouling target (Arabshahi et al. 2021; Gaudêncio and Pereira 2022) with potential in the discovery of new ecofriendly antifouling compounds (Zhang et al. 2014; Quémener et al. 2022).

This study reports on dereplication, in silico and field studies, ecotoxicological profiles and antifouling potential of the metabolites from *M. sarasinorum*, providing insights for the development of novel and effective eco-friendly antifoulants.

MATERIALS AND METHODS

Study area

The *M. sarasinorum* sponges were hand-collected using scuba from Kawaluso and Mahumu in Sangihe Islands District, North Sulawesi, Indonesia (Figure 1), in June 2019, at a depth of 7-15 meters. The specimens were prepared, stored, and evaluated using the same method we previously reported (Balansa et al. 2024). The field study was carried out over 31 days in June and July 2023 at the mariculture facility of Politeknik Negeri Nusa Utara in Teluk Talengen, Sangihe Islands. Antibacterial assays and metabolomic analyses were conducted at Justus Liebig University of Giessen, Germany.

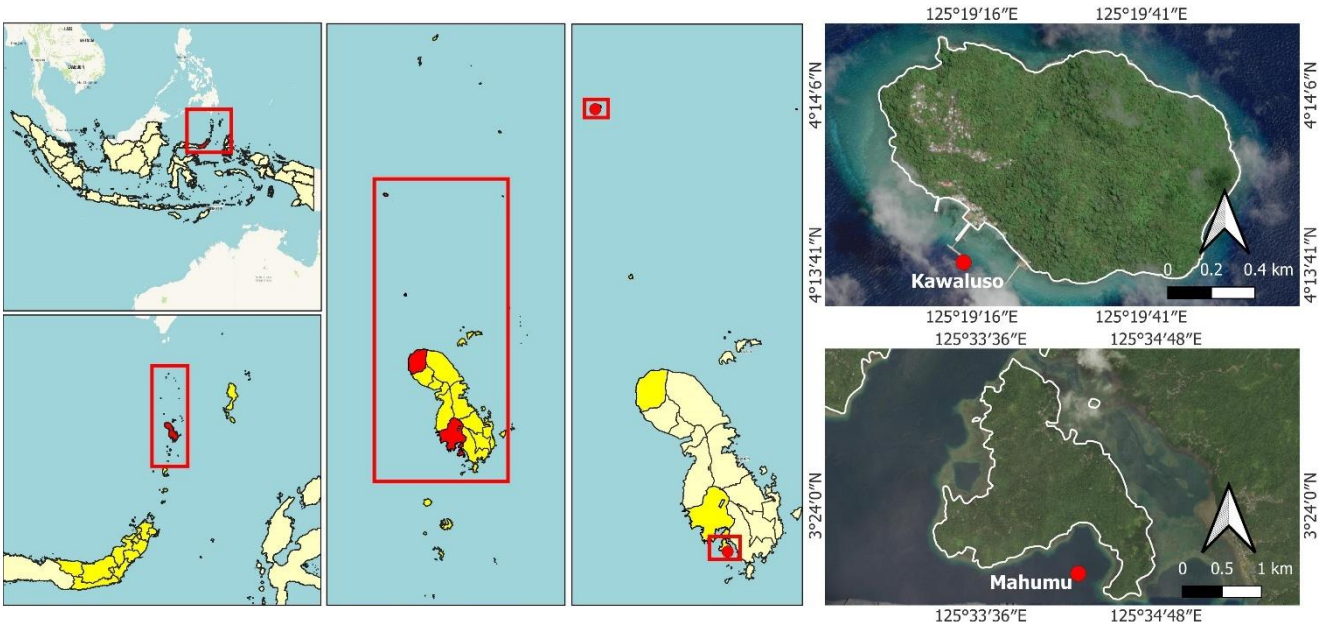

Figure 1. Locations of the sampling sites for *Melophlus sarasinorum* at point 1 (4° 13' 56" N, 125° 19' 29" E) and point 2 (3° 23' 33" N, 125° 34' 16.0" E) in Kawaluso and Mahumu in Sangihe Islands, North Sulawesi, Indonesia

Procedures

Sample collection and identification

The specimen, weighing 50 g (wet weight), was cut into smaller pieces and solar-dried for 6 hours, similar to our previous report (Balansa et al. 2024). The sponge was identified using our previously reported method (Rieuwpassa et al. 2023), with a slight modification to the acid digestion method (Hooper and van Soest 2022). Soon after the specimen was exposed to air, its color turned from light brown to reddish brown. The sponge was egg-shaped with a central osculum supported by a three-legged structure. Further analysis showed the presence of megascleres in the form of oxea spicules, measuring between 498.22 mm and 515.16 mm in length. These morphological characteristics were in accordance with *M. sarasinorum* (Hooper and van Soest 2002; Riyanti et al. 2020b).

Antimicrobial and metabolomic studies

Micro broth dilution assays were conducted in 384-well microtiter plates against *Escherichia coli* ATCC 35218, *Staphylococcus aureus* ATCC33592, and *Pseudomonas aeruginosa* ATCC using gentamycin as a positive control. UPLC-MS/MS data collection and analysis was performed on a UPLC-HRMS/MS system (Bruker, Billerica, MA, USA) ESI-qTOF-UHRMS. Molecular networking analysis was performed online using the GNPS infrastructure (Aron et al. 2020).

Molecular docking

The target protein, AChE (PDB ID: 6G1U), was obtained from the Protein Data Bank (http://www.rcsb.org/pdb) at a resolution of 2.85 Å. This crystal structure was chosen due to the conserved nature of the AChE active site across species (Sussman et al. 1991). Its suitability for identifying broad-spectrum antifouling inhibitors was further validated using *Crassostrea gigas* (Thunberg, 1793) AChE (Arabshahi et al. 2021), ensuring an accurate representation of the enzyme. The 3D sdf files of all ligands (sarasinosides A1-A3 (**1**-**3**), D (**4**), L (**5**), M (**6**), M2 (**7**), synoxalidinones A (**8**), C (**9**), irgarol_1501 (**10**), seanin_211 (**11**), econea® (12) and selektope® (**13**) were downloaded from PubChem. PyRx molecular docking software and AutoDock Wizard accomplished the autodocking of ligands. Tests were conducted in nine replicates with the best Root Mean Square Deviations (RMSDs) (zero) and best poses (the lowest docking score) used.

Antifouling study

Sponge powder was obtained from *M. sarasinorum* collected by scuba diving at a depth of 5 meters in Mahumu, Sangihe Islands, Indonesia. The collected sponge was frozen, air-dried, and then ground into a fine powder using a blender. Polyethylene nets (10 × 15 cm^2) with a 1-inch mesh size were prepared from prime-grade high-density polyethylene. Antifouling agents were prepared in triplicate by separately mixing 1, 2, and 3 mg of sponge powder with 10 mL of epoxy resin to achieve 1:1, 1:2 and 1:3 sponge powder/epoxy mixture, respectively. The mixture was evenly applied to the polyethylene nets, including their nodes, using a brush and allowed to dry for 48 hours. The treated nets were then attached to the upper sides of cages and buoys, simulating a floating fish farm net configuration. Subsequently, they were immersed in the sea for 30 days. The same methodologies have been previously reported by Balansa et al. (2024).

Statistical analysis

To evaluate the effectiveness of the *M. sarasinorum* extract as an antifouling agent for polyethylene nets, we used a formula, software, and data analysis previously reported by Balansa et al. (2024). In short, determining the antifouling activity involved measuring the final weight of the nets and subtracting from them the initial weight of each net observed after one month (lighter nets indicate stronger antifouling activity). The field study results were analyzed using a complete randomized design Analysis of Variance (ANOVA) under the Statistical Package for Social Science (SPSS) 16.0 Program. In addition, we applied the Fisher's Exact Test to compare the activities of sarasinosides using GraphPad (available at https://www.graphpad.com/quickcalcs/contingency). Beneficial and harmful scores were assigned based on specific criteria related to their efficacy and safety profiles.

Ecotoxicological evaluation

To assess the potential environmental impact of sarasinosides, AChE inhibitors, and commercial antifoulants, we predicted several key physicochemical properties using the U.S. EPA's EPI Suite™ software (KOWWIN™, KOCWIN™, BCFBAF™, BIOWIN™, and ECOSAR™) (Card et al. 2017). They include Log K_{ow} (Octanol-Water Partition Coefficient) which estimates bioaccumulation potential with values ≥3.0 suggesting a tendency to accumulate in organisms (ECHA 2021; Vilas-Boas et al. 2021). Log K_{oc} (Soil/Sediment Adsorption Coefficient) estimates binding to soil and sediment; values ≤3.0 suggest low adsorption, while ≥3.5 suggests medium adsorption (ECHA 2017; Vilas-Boas et al. 2023). Log BAF/BCF (Bioaccumulation/Bioconcentration Factor) estimates compound concentration in fish tissues; values >3.0 suggest high bioaccumulation (Mackay and Fraser 2000; Kobayashi 2021). Biotransformation Half-Life (BHL) estimates how quickly a compound breaks down; values ≤1 day indicate rapid breakdown, ≥1 to 30 days moderate, and ≥30 days persistent (Papa, 2018). Water Solubility is classified as low (<1 mg/mL), moderate (1-100 mg/mL), or high (>100 mg/mL) (Ronald Ney, 1995). Referred also as K_{ow}, LogP indicates absorption of a substance/substances by living organisms also it is referred as K_{ow} with negative and positive values indicating higher affinity for aqueous (1) and lipid (0) phases respectively (Bhal 2007). Biodegradability (via Biowin5) with values ≥0.5 = 1 (Yes) indicating fast biodegradability (Yes), while ≤0.5 = 0 (No) suggesting slow biodegradability. We used these thresholds to create a binary scoring system (0 = No, 1 = Yes) for evaluating overall environmental risk.

RESULTS AND DISCUSSION

Previous studies have identified numerous antifouling compounds derived from various marine organisms, particularly sponges (Stowe et al. 2011; Puentes et al. 2014; Qian et al. 2015). While the identification of new compounds is paramount, past experimental studies have neglected the connection between antifouling activity and antibacterial activity. Furthermore, the cytotoxicity and potential environmental implications for these novel agents remain largely unreported. In contrast, this study comprehensively assessed the antibacterial activity of metabolites identified from the sponge *M. sarasinorum*. It evaluated their antifouling activity through molecular docking to a known antifouling target, acetylcholinesterase (AChE) (Arabshahi et al. 2021), and conducted a field study to confirm the antifouling efficacy. This integrated approach provides compelling evidence supporting the potential of sarasinoside-type compounds as candidates for eco-friendly antifouling agents.

Antimicrobial and metabolomic studies

Our quest began by evaluating the antibacterial activity and metabolomic profiles of 63 sponges from the Sangihe Islands. Our attention was drawn to the metabolites from two specimens collected from Kawaluso (KW_01) and Mahumu (MS_09), morphologically identified as *M. sarasinorum* with underwater picture and megascleres oxea typed spicules measuring ±245-284 and ±242-303 μm for both specimens respectively (Figure 2). While both extracts were inactive against the Gram-negative bacteria *Escherichia coli* 35218 TEM1 only the extract of *M. sarasinorum* from Kawaluso exerted moderate antimicrobial activity against *Staphylococcus aureus* ATTC33592 MRSA inhibiting 98%, 87%, and 33% (>80% is considered active) of the concentration of 10, 5 and 0.25 mg/mL respectively (Table 1).

The molecular networking analysis revealed a large cluster in which several nodes were annotated as members of the Sarasinoside family, namely *m/z* 1303.6467 ± 0.005 $[M+H]^+$ ($C_{62}H_{98}N_2O_{27}$), *m/z* 1291.6777 ± 0.005 $[M+H]^+$ ($C_{62}H_{102}N_2O_{26}$), *m/z* 1289.6591±0.005 $[M+H]^+$ ($C_{62}H_{100}N_2O_{26}$), *m/z* 1287.6466±0.005 $[M+H]^+$ ($C_{62}H_{98}N_2O_{26}$), *m/z* 1273.6657 ± 0.005 $[M+H]^+$ ($C_{62}H_{100}N_2O_{25}$), *m/z* 1321.6515 ± 0.005 $[M+H]^+$ ($C_{62}H_{100}N_2O_{28}$), (Figure 3, Figure 4.A-4.E). Manual inspection of the MS/MS spectra confirmed the structural identity of Sarasinosides A1-level 2 annotation (Figure 3), A4/5, D, L and M2 (Figure 4.A-4.E) (Sumner et al. 2007). Also, the extract of *M. sarasinorum* showed an additional signal at *m/z* of 337.9022 ± 0.005 $[M+H]^+$ ($C_9H_9Br_2NO_3$) annotated as 3,5-bromotyrosine-level 2 annotation (Figure 4.F).

It is well documented that sarasinosides are frequently isolated from the marine sponge *M. sarasinorum* (Kobayashi et al. 1991; Dai et al. 2005; Kalinin et al. 2012; O'Brien et al. 2023). However, the detection of 3.5-dibromotyrosine is the first time from *M. sarasinorum*, as this compound has previously been reported from sponges belonging to Aplysinellidae, Aplysinidae, Ianthellidae, and Pseudoceratinidae families (Ferreira Montenegro et al. 2024).

Many triterpene glycosides derived from sponges (e.g., erylosides, sokodosides, caminosides, and sarasinoside J) are reported to owe their antifouling activity to their antibacterial properties (Kalinin et al. 2012). The antifouling process involves the initial colonization of the surface by a microbial biofilm, which subsequently triggers the recruitment and attachment of marine larvae, leading to the development of adult macrofouling on the surface of submerged marine structures (Gomez-Banderas 2022); therefore, compounds that can prevent biofilm formation are potentially proactive measures for remediating macrofouling (Kalinin et al. 2012; Tadesse et al. 2014). The relationship between the antibacterial and antifouling properties of triterpene glycosides has been studied in sponges, such as *Erylus formosus* (Sollas, 1886) and *Ectyoplasia ferox* (Duchassaing & Michelotti, 1864) (Kalinin et al. 2012), resulting in the discovery of erylosides, sokodosides, caminosides, and sarasinoside J (Kalinin et al. 2012). Nevertheless, this relationship remains largely unexplored with the exception for sarasinoside J from *M. sarasinorum*, prompting us to further investigate the antifouling and antimicrobial properties of other sarasinoside analogues on polyethylene nets in a mariculture facility.

Field study

To investigate the antifouling potential of the previously dereplicated sarasinosides from *M. sarasinorum* collected in Sangihe, a 31-day field study was conducted in a mariculture environment in Talengen Bay, Sangihe Islands, utilizing powdered *M. sarasinorum* collected from Mahumu. This initial investigation aimed to evaluate in a field setting, the efficacy of the sponge powder against marine biofouling at varying concentrations. This approach acknowledges the influence of surface characteristics, as rougher surfaces are known to exhibit a greater propensity for biofouling compared to smoother structures (Yu et al. 2016; Nogueira et al. 2017; Abdalla et al. 2021). Furthermore, the complexity and intricate nature of biofouling communities suggest that the application of a single, pure compound is unlikely to be wholly effective (Chen et al. 2023, 2024a). Instead, these studies argue that successful biofouling mitigation likely relies on the synergistic effects of multiple compounds (Chen et al. 2023, 2024a).

Table 1. Antibacterial activity (%) of *Melophlus sarasinorum* from Kawaluso (KW_01) and Mahumu (MS_09)

Sample	***S. aureus* ATCC 33592 MRSA (mL)**			***E. coli* ATCC 35218 TEM-1 (mL)**		
	10	**0.5**	**0.25**	**10**	**0.5**	**0.25**
KW_01	98	87	33	–19	–12	-6
MS_09	–1	6	9	–12	–16	-11

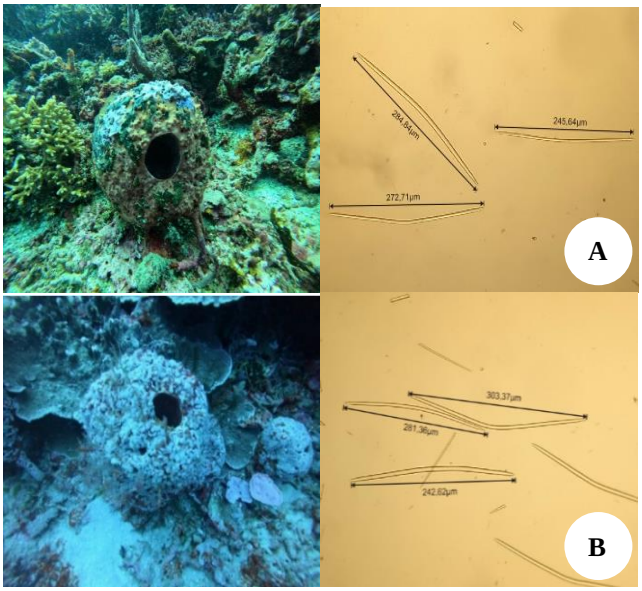

Figure 2. Underwated images and oxea spicules of *Melophlus sarasinorum* from: A. Mahumu; B. Kawaluso Islands

The field study revealed a significant reduction in fouling organisms on nets treated with powder of *M. sarasinorum* collected from Mahumu Island compared to untreated nets. The untreated nets (negative control) exhibited the highest fouling, accumulating a total weight of 48.0 g (Figure 5, A5/B5). In comparison, nets treated solely with epoxy resin displayed less fouling, with a total weight of 42.66 g (Figure 5, A4/B4). Moreover, nets treated with 1:1, 1:2, and 1:3 (sponge powder/epoxy resin) experienced varying degrees of fouling, resulting in total weights of 22.0, 32.0, and 36.6 g, respectively (Figure 5, A1/B1; A2/B2; A3/B3). However, it is worth noting that the values did not reflect the actual mass of bioactive compounds, which could be as low as 0.0172% and 0.160% for minor and major bioactive compounds from their crude extract (Balansa 2014). These findings revealed an inverse relationship between concentration and antifouling efficacy, with the most diluted treatment (1:1) demonstrating the strongest antifouling activity and the highest concentration exhibiting the weakest effect (Figure 5, A1/B1).

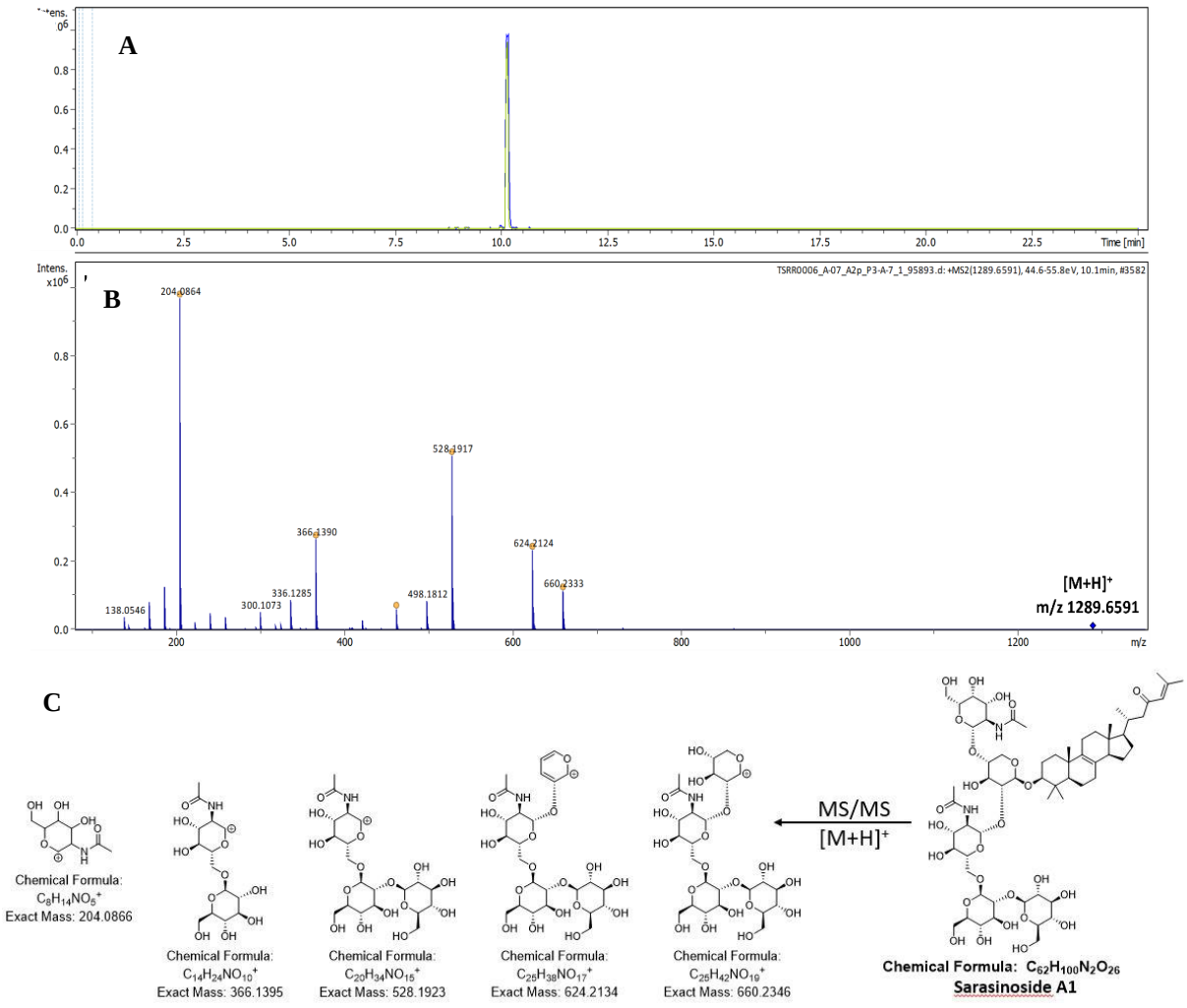

Figure 3. A. Overlaid extracted ion chromatograms at *m/z* 1288.6564±0.005 corresponding to the $[M+H]^+$ ion with formula $C_{62}H_{100}N_2O_{26}$ (assigned as Sarasinoside A1) from Kawaluso sponge (blue), Mahumu sponge (green) extracts; B. Fragmentation spectrum of the precursor ion at *m/z* 1289.6591±0.005 $[M+H]^+$; C. Structures of sarasinoside A1 and putative structures of fragmentation ions explaining the experimental MS/MS spectrum

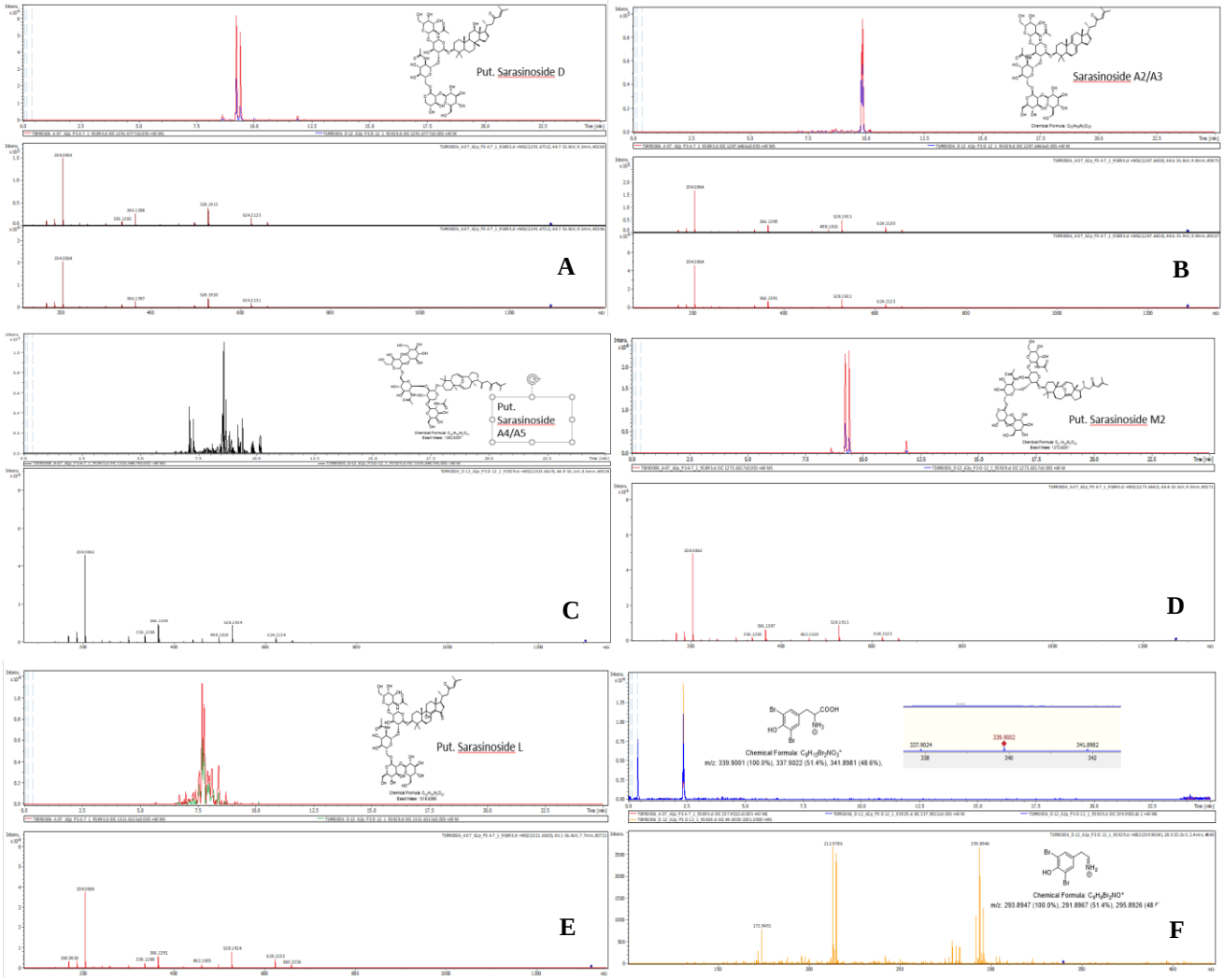

Figure 4. Extracted ion chromatograms MS/MS spectra of sarasinosides D with *m/z* 1291.6777±0.005 $[M+H]^+$ ($C_{62}H_{102}N_2O_{26}$) and A2/A3 with *m/z* 1287.6466±0.005 $[M+H]^+$ ($C_{62}H_{98}N_2O_{26}$) (A-B), sarasinosides A4/A5 with *m/z* 1303.6467±0.005 $[M+H]^+$ ($C_{62}H_{98}N_2O_{27}$) and M2 with *m/z* 1273.6657±0.005 $[M+H]^+$ ($C_{62}H_{100}N_2O_{25}$) (C-D), sarasinoside L with *m/z* 1321.6515±0.005 [M+H]+ ($C_{62}H_{100}N_2O_{28}$) from Kawaluso (KW_01) and Mahumu (MS_01) (E) along with 3,5-dibromotyrosine of *M. sarasinorum* from Kawaluso with *m/z* 337.9024±0.005 $[M+H]^+$ ($C_9H_9Br_2O_3$) (F)

The results also indicate that the surface characteristics of the nets influence biofouling activity. Nets treated with epoxy resin alone (Figure 5, A4/B4) harbored fewer biofouling organisms compared to untreated nets (Figure 5, A5/B5). Polyethylene netting is particularly susceptible to biofouling due to its coarse texture (Hodson et al. 1997; Kartal and Sarıışık 2022). In contrast, the application of epoxy resin results in a smooth, water-resistant coating that deters the attachment of (micro)organisms. Similarly, nets treated with higher concentrations of sponge powder/epoxy resin 1:2 (Figure 5, A2/B2) and 1:3 (Figure 5, A3/B3) were more heavily fouled compared to those treated with the lowest concentration (1:1). This suggests that an optimal concentration of the extract is crucial for maximizing antifouling efficacy, and both cases demonstrate the impact of substrate structure on anti-biofouling activity.

These results corroborate our previous findings on the antifouling activity of agelasine-type compounds (Balansa et al. 2024) and are consistent with earlier studies reporting that larger and rougher surface areas are more prone to marine biofouling (Hodson et al. 1997; Kartal and Sarıışık 2022). One explanation for this trend is that rough surfaces can act as defensive shields against shear forces, capable of preventing bacterial detachment from the substrate (Wassmann et al. 2017), facilitating bacterial attachment, proliferation and biofilm formation of *Staphylococcus epidermidis*, *Pseudomonas aeruginosa*, *Ralstonia pickettii*, *Streptococci* etc. (Xing et al. 2015; Yu et al. 2016; Nogueira et al. 2017; James et al. 2019; Yao et al. 2020; Abdalla et al. 2021; Zheng et al. 2021).

The statistical analysis demonstrated that all treatments (100, 200, and 300 mg/mL) differed significantly from both the untreated nets and the net treated with epoxy resin alone ($p<0.05$) (Table 2). A post-hoc Duncan test further confirmed that net treated with 100 mg/mL was significantly different from those treated with 200 and 300 mg/mL (Table 3).

Molecular docking

While studies have associated sarasinoside J with antifouling and antimicrobial activity (Kalinin et al. 2012; Ivanchina and Kalanin 2023), the precise mechanisms underlying sarasinoside bioactivity are not fully elucidated. In addition to their demonstrated anticancer effects, the potential for other modes of action warrants further investigation. Sarasinoside A1, for example, exhibited anticancer activity by disrupting cell signaling pathways mediated by Rap GTPase activation during epithelial-to-mesenchymal transition (Austin et al. 2013; Pérez-Aguilar et al. 2023). This suggests that sarasinosides may possess diverse mechanisms, potentially exhibiting dual antifouling and anticancer activity rather than the known antimicrobial and antifouling effects. This possibility is supported by the observation that sarasinosides exhibit greater cytotoxic than antimicrobial activity (Kalinin et al. 2012; Ivanchina and Kalanin 2023). Furthermore, increasing evidence highlights the substantial connections between cancer development and cholinergic signaling, particularly the involvement of acetylcholinesterase (AChE) in acetylcholine hydrolysis, catalytic function, and apoptosis induction (Aronowitz et al. 2022; Pérez-Aguilar et al. 2023). Intriguingly, both commercial antifoulants (e.g., diuron, irgarol 1051) and marine-derived AChE inhibitors (e.g., territrem, synoxalidinones A and C, butyrolactone derivatives) have been experimentally shown to inhibit AChE in *Artemia salina* (Linnaeus, 1758) and barnacle larvae, respectively (Nong et al. 2014; Lee et al. 2017). Consequently, we hypothesize that sarasinosides may disrupt the cholinergic system of fouling organisms by inhibiting AChE activity. Therefore, to further explore the antifouling potential of sarasinosides, we will investigate AChE inhibition as a potential mechanism underlying their antifouling activity through molecular docking.

Molecular docking studies revealed distinct interactions between sarasinosides, AChE inhibitors and commercial antifouling (Figure 6). Compounds **2**, **3**, **5**, and **6** were found to bind to site 1 on chain B of the 6G1U structure, while compounds **1**, **4**, and **7** interacted with site 11 on chain A of the receptor (Figure 7) with binding affinities of –8.9, –9.6, –9.0, –8.9, –10.0, –8.9 and –9.4 Kcal/mol for **1-7** respectively, rivaling or surpassing both AChE inhibitors (**8**, **9**) and antifouling commercial (**10-13**). Unlike the AChE inhibitors and commercial antifoulants, which showed interaction with amino acid residues of the active site of the AChE, none of the sarasinosides formed interactions with the amino acid encircling the active site of AChE (Table 4, Figure 8). The active site, known as the gorge site, is encircled by 14 amino acid residues, including Phe75, Phe288, Phe330, Phe331, Trp44, Trp84, Tyr130, Trp233, Trp432, Tyr70, Tyr121, Trp279, Tyr334, and Tyr442. AChE features both a Catalytic Anionic Site (CAS) at the receptor's opening, characterized byTrp789, and a Peripheral Anionic Site (PAS) at the base of the receptor, marked by Trp84 (Luque and Muñoz-Torrero 2024). In addition to these primary binding sites, other regions may also serve as allosteric sites where ligands can bind and modulate AChE activity (Johnson and Moore 2006; Marcelo et al. 2013; Roca et al. 2018; Luque and Muñoz-Torrero 2024).

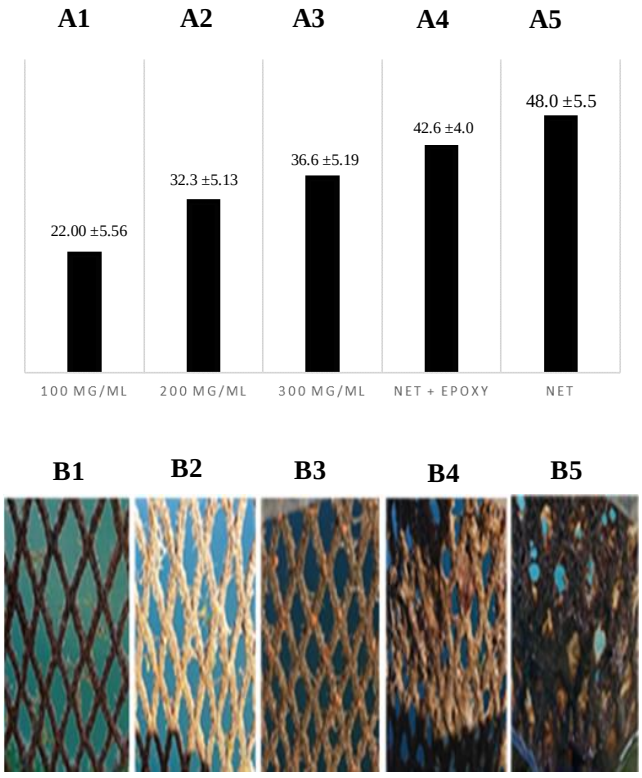

Figure 5. Field study results depicting the final wet weights of the untreated net (A4/B4) and those treated with 1:1 (A1/B1), 1:2 (A2/B2), or 1:3 (A3/B3) *Melophlus sarasinorum* powder/epoxy resin mixture, alongside the positive control (A4/B4), epoxy resin (A5/B5)

Table 3. Duncan Test

Treatment	N	Subset for alpha = 0.05		
		1	2	3
1:1	3	22		
1:2	3		34,33333	
1:3	3		36	
net+epo	3		41,66667	41,66667
net	3			48
Sig.		1	0,109852	0,143928

Note: Means for groups in homogeneous subsets are displayed

Table 2. Anova One-Way

	Sum of squares	df	Mean square	F
Between Groups	1122,267	4	280,5667	11,72284
Within Groups	239,3333	10	23,93333	
Total	1361,6	14		

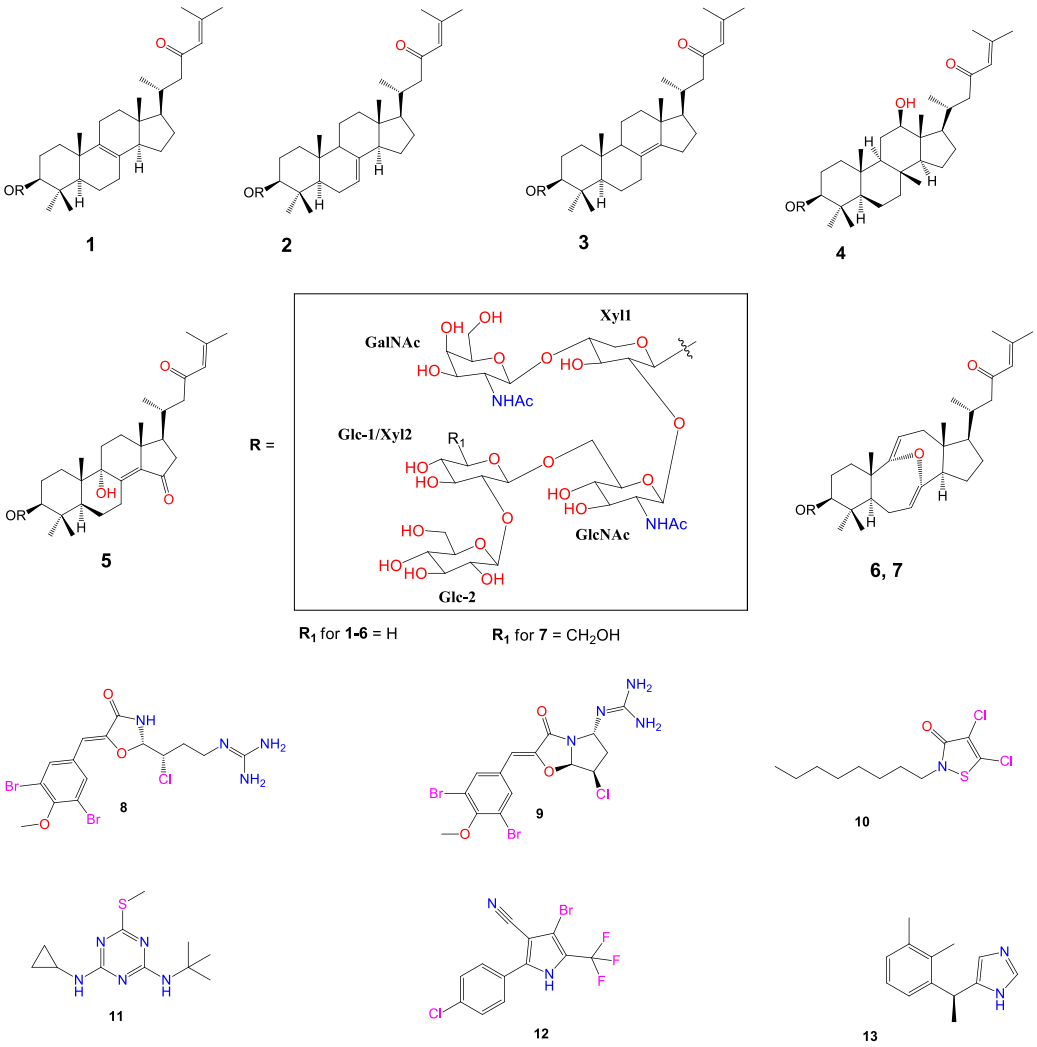

Figure 6. The dereplicated structures of sarasinosides A1-A3 (**1-3**), D (**4**), L (**5**), M2 (**6**), A4/A5/M (**7**), alongside their sugar types N-acetyl galactosamine (GalNAc), xylose 1 (xyl1), xylose 2 (Xyl2), glucose 1 (Glc1), glucose 2 (Glc2), N-acetyl-D-glucosamine (GlcNAc), AChE inhibitors, synoxazolidinones A (**8**) and C (**9**), and commercial antifouling seanine_211 (**10**), irgarol_1501 (**11**), econea® (**12**) and selektope® (**13**)

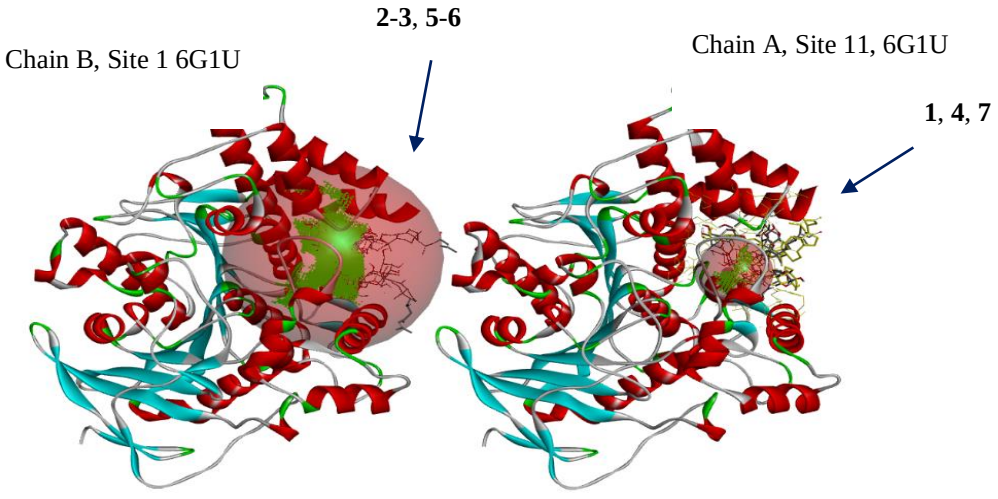

Figure 7. Predicted binding sites of sarasinosides D and A2 on 6G1U, a two-chain fragment of AChE: A. Compounds **2-3** and **5-6** bind to site 1 on chain B; while B. Compounds **1**, **4**, and **7** to site **11** on chain A

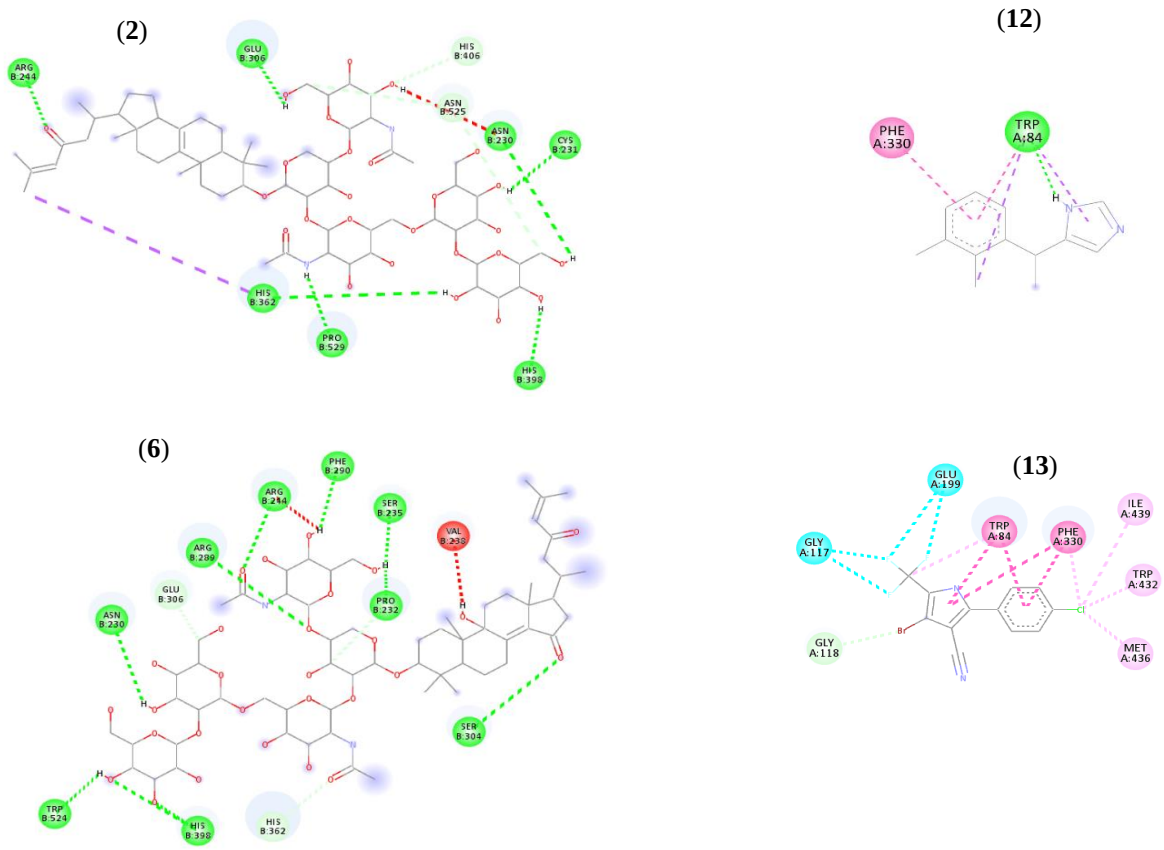

Figure 8. Two-dimensional ligand-protein interaction between sarasinosides A2 (**2**) and M2 (**6**), econea® (**12**) and selektope® (**13**)

Table 4. Docking results of metabolites from *Melophlus sarasinorum* (1-7), synoxazolidinones A and C (8, 9), seanin_211 (10), irgarol_1501 (11), Selektope® (12), and Econea® (13)

Ligands	Binding affinities	Important interaction
Sarasinoside A1 (**1**)	–8.9 (B)	Arg244, Pro529, Cys231, Asn230, His398, His362, Glu306 (hydrogen bond) Asn525, His362 (carbon-hydrogen bond)
Sarasinoside A2 (**2**)	–9.6 (A)	Ser237, Ser237, Ser237, Ser235, Glu240, Ser235, Ser235, UNK1, UNK1, UNK1, Asn525, His362, His398, L u386 (hydrogen bonding), Leu366 (hydrophobic interaction)
Sarasinoside A3 (**3**)	–9.0 (B)	Arg244, Lys410, Glu306, Ser235, UNK1, UNK1, UNK1, Arg289, UNK1, Asn525, Pro232, Ser235 (hydrogen bond), Pro529 (hydrophobic interaction)
Sarasinoside D (**4**)	–8.9 (B)	Asn310, Ser235, Trp524, UNK1, Trp524, Asn525, Glu306, UNK1, UNK1, His406, UNK1, (hydrogen bond) Pro283, Arg289, Pro361, Phe284 (hydrophobic interaction)
Sarasinoside L (**5**)	–10.0 (A)	Arg244, Arg289, Ser304, His398, His398, Asn230, Phe290, Pro232, Ser235, (hydrogen bond), His362, Pro232, Glu306, UNK1 (hydrophobic interaction)
Sarasinoside M2 (**6**)	–8.9 (B)	UNK1, Glu240, UNK1, Glu306, His362, UNK1, Ser304, His406 (hydrogen bond).
Sarasinoside M (**7**)	–9.4 (A)	Ala460, Ans230, Arg289, UNK1, Tyr458, Glu240, Pro403 (hydrogen bond), Pro529 (hydrophobic interaction)
Synoxalidinone A (**8**)	–9.5 (A)	Tyr121, Gly335, Trp279, Trp279, Leu282, Trp279, Trp279
Synoxalidinone C (**9**)	–8.9 (A)	Asp285, Trp279, Leu282, Leu282, Trp279, Trp279, Ile287, Try70, Trp279, Trp279
Seanin_211 (**10**)	–5.3 (A)	His398, His398, His398, His362, Pro232, Pro403, His362, His406, His406, Pro232, Pro529
Irgarol_1501 (**11**)	–5.5 (A)	Ser286, Trp279, Trp279, Trp279, Leu282, Phe330, Phe331
Selektope® (**12**)	–9.3 (A)	Trp84 (hydrogen bond), Trp84, Trp84, Trp84, Phe330 (hydrophobic interaction)
Econea® (**13**)	–9.9 (A)	Gly118 (hydrogen bond), Gly117, Gly117, Gly199, Trp84 (halogen bond), Trp84, Trp84, Phe330, Trp84, Phe330, Met436, Ile439, Trp84, Trpu84, Phe330, Trp432 (hydrophobic interaction)

Our results show that while the AChE-specific inhibitors synoxalidinones A (**8**) and C (**9**) and the commercial antifoulants, irgarol_1501 (**11**), econea® (**12**) and selektope® (**12**) seem to bind to the active site of AChE as they bound to a few amino acid residues such as Trp84, all dereplicated sarasinosides seem to bind to allosteric site (Table 4, Figure 8). This is because synoxalidinones A and C, irgarol_1501, selektope® and econea® formed multiple bonds with Trp279, an amino acid in the CAS indicating strong binding affinities, with the exception of irgarol_1501, which showed lower binding affinity despite having multiple interactions with other amino acid residues, such as Phe330 and Phe331 (Table 4, Figure 8). In contrast, seanin_211 and the sarasinosides did not interact with active site residues but were able to form hydrogen bonds to Ser235, His362, His398 (sarasinosides A2 and L) or with Arg289, Tyr458, Pro403 (sarasinoside M) (Table 4; Figure 7). These findings suggest that sarasinosides did not bind to the active site of AChE but likely bound to putative allosteric sites on AChE. This finding aligns with results from previous studies reporting the presence of different ligand interaction sites other than the active site of AChE (Johonson et al. 2006; Marcelo et al. 2013; Roca et al. 2018; Luque and Muñoz-Torrero 2024).

Toxicity test

To predict the environmental risk associated with sarasinosides, AChE inhibitors, and commercial antifouling agents, we converted continuous data (Table 5) derived from EPI Suite™ (Card et al. 2017) into a binary scoring system. Each ecotoxicological parameter was assigned a score of 1 (indicating a more favorable characteristic, based on the established thresholds mentioned earlier in the method section) or 0 (indicating a less favorable characteristic). To facilitate comparison of the overall environmental profiles, a total score was calculated for each compound. The total score represents the proportion of favorable characteristics exhibited by the compound, as determined by the binary scoring system in Table 6. The total score was calculated as follows: Total score = (Number of Favorable Characteristics)/ (Total Number of Parameters). This approach provides a standardized measure of the proportion of favorable characteristics, allowing for easier comparison across compounds. The total score ranges from 0 to 1, with higher scores indicating a potentially more favorable environmental profile. To predict the significance of differences in ecotoxicological impact between compounds, Fisher's exact test was performed, using a 2 × 2 contingency table to compare the number of favorable characteristics (outcome 1) and unfavorable characteristics (outcome 2) for the compounds in comparison (Table 7). Therefore, this approach provides a simplified, semi-quantitative indication of potential environmental impact, based on the assumption that each parameter contributes equally to the overall environmental profile.

The results indicated that the water solubility of the sarasinosides, with most of them exhibiting low solubility, ranging from 8.901×10^{-4} to 1.06×10^{-1} mg/mL, has significant implications on the discovery of ecofriendly antifoulants (Vilas-Boas et al. 2021). Sarasinoside D (**4**) was an exception, demonstrating moderate water solubility at 5.63 mg/mL. Similarly, the antifouling agent econea® (12) showed low water solubility at 0.3364 mg/mL. In contrast, synoxazolidinones A (8) and C (**9**), seanin_211 (**10**), irgarol_1501 (**11**), and selektope® (**13**) exhibited moderate solubility, with values of 34.4, 13.3, 13.4, and 7.52 mg/mL, respectively (Table 6). The findings underscore the importance of considering water solubility in the environmental fate of these compounds. It is well-established that compounds with high water solubility are less likely to be adsorbed into sediments and tend to bioaccumulate in fatty tissues (van Gestel et al. 1985). Conversely, compounds with low water solubility are likely to bind tightly to the hydrophobic matrices of marine coatings, ensuring a sustained release into the aquatic environment (Vilas-Boas et al. 2021).

Table 5. Toxicity test results obtained from EPI Suite™ on compounds **1-13**

Compound	Water Solubility (mg/mL)	Fish 96 hr LC_{50} (mg/L)	Daphnid 48 hr LC_{50} (mg/L)	Green Algae 96 hr EC_{50}	Log K_{ow} L/kg (ww)	Log BCF L/kg (ww)	Log BAF L/kg (ww)	BHL	Log K_{oc}	Biod. Fast/ Biowin5 (Y/N)	LogP
Sarasinoside A1 (**1**)	1.49×10^{-3}	2.16×10^{4}	2.36×10^{4}	1.01×10^{4}	0.41	3.16	0.941	$3.05x10^{-4}$	-0.17	0.2915/N	-2.68
Sarasinoside A2 (**2**)	4.41×10^{-4}	1.05×10^{5}	1.51×10^{5}	5.43×10^{4}	-0.49	3.16	0.899	$1.66x10^{-4}$	-0.21	0.1176/N	-2.90
Sarasinoside A3 (**3**)	8.90×10^{-4}	25027.0	28080.0	11857.0	0.32	3.16	0.933	$2.84x10^{-3}$	-0.21	0.0620/N	-2.76
Sarasinoside D (**4**)	5.63	5.24×10^{8}	3.43×10^{9}	4.69×10^{8}	-5.43	3.16	0.893	$1.74x10^{-5}$	-2.83	0.1777/N	-3.82
Sarasinoside L (**5**)	0.1061	2.27×10^{7}	8.46×10^{7}	1.66×10^{7}	-3.54	3.16	0.893	$4.05x10^{-5}$	-2.15	0.3555/N	-4.39
Sarasinoside M (**6**)	1.37×10^{-4}	46855	58623.5	2.31×10^{7}	-0.03	3.16	0.911	$1.91x10^{-4}$	-0.47	0.2254/N	-2.83
Sarasinoside M2 (**7**)	2.30×10^{-4}	47221	59407.0	23315.0	-0.05	3.16	0.911	$3.15x10^{-3}$	-0.41	0.1115/N	-2.19
Synoxazolidinone A (**8**)	13.3	88306	10589.0	8635.0	2.05	10.5	0.244	11	1.95	0.7121/N	2.50
Synoxazolidinone C (**9**)	34.4	1.78×10^{5}	2.02×10^{4}	1.83×10^{4}	1.59	5.16	1.45	4.91	1.67	0.0211/N	2.35
Seanin_211 (**10**)	13.4	0.051	0.079	0.122	3.59	109	1.03	211	2.88	0.2210/N	4.57
Irgarol_1501 (**11**)	7.52	2.12	3.68	0.025	4.74	14.6	0.257	17	2.63	0.1190/N	2.37
Econea® a (**12**)	0.3364	0.034	2.677	0.149	4.69	575	3790	16.3	4.54	0.0019.N	4.98
Selektope® (**13**)	23.56	0.65	0.51	0.095	3.83	155.4	331.0	1.48	3.83	0.2310.N	3.18

Table 6. Beneficial properties of compounds **1-13** calculated using a binary system

Compound	Water solubility mg/mL	Fish 96 hr LC_{50} mg/L	Daphnid 48 hr LC_{50} mg/L	Green Algae 96 hr EC_{50}	Log K_{ow} L/kg ww	Log BCF L/kg ww	Log BAF L/kg ww	BHL	K_{oc} win/ Log Koc	Biod. fast/ Biowin5	LogP	Total score
Sarasinoside A1 (**1**)	1	1	1	1	1	1	1	1	1	0	1	0.91
Sarasinoside A2 (**2**)	1	1	1	1	1	1	1	1	1	0	1	0.91
Sarasinoside A3 (**3**)	1	1	1	1	1	1	1	1	1	0	1	0.91
Sarasinoside D (**4**)	0	1	1	1	1	1	1	1	1	0	1	0.81
Sarasinoside L (**5**)	1	1	1	1	1	1	1	1	1	0	1	0.91
Sarasinoside M (**6**)	1	1	1	1	1	1	1	1	1	0	1	0.91
Sarasinoside M2 (**7**)	1	1	1	1	1	1	1	1	1	0	1	0.91
Synoxazolidinone A (**8**)	0	1	1	1	1	0	1	0	1	0	0	0.55
Synoxazolidinone C (**9**)	0	1	1	1	1	0	1	0	1	0	0	0.55
Seanin_211 (**10**)	0	0	0	0	0	0	1	0	1	0	0	0.18
Irgarol_1501 (**11**)	0	1	1	0	0	0	1	0	1	0	0	0.36
Econea® (**12**)	1	0	1	0	0	0	0	0	1	0	0	0.27
Selektope® (**13**)	0	0	0	0	0	0	0	1	0	0	0	0.09

Table 7. 2 × 2 contingency table of fisher exact test among ligands

Comparison	Outcome 1	Outcome 2	Total	p-value	Statistical significance
Sarasinoside A1 (**1**)	10	1	11	0.1486	Not statistically significant
Synoxazolidinone A (**8**)	6	5	11		
Sarasinoside A1 (**1**)	10	1	11	0.1486	Not statistically significant
Synoxazolidinone C (**9**)	6	5	11		
Sarasinoside A1 (1) vs Seanin_211 (**10**)	10	1	11	0.0019**	Very significantly
	2	9	11		
Sarasinoside A1 (1) vs irgarol_1501 (**11**)	10	1	11	0.0237*	Significantly different
	4	7	11		
Sarasinoside A1 (1) vs econea® (**12**)	10	1	11	0.0075*	Significantly different
	3	8	11		
Sarasinoside A1 (1) vas selektope® (**13**)	10	1	11	0.0003**	Extremely significant
	1	10	11		

These findings suggest that sarasinosides A1-A3 (**1-3**), D (**4**), L (**5**), M (**6**), and M2 (**7**) adhere more effectively to coating materials than both AChE inhibitors and commercial antifouling agents, a key property for successful antifouling performance (Vilas-Boas et al. 2021). The water solubility of sarasinosides A1-A3, L, M, and M2 was in the same order of magnitude as that of econea®. In contrast, sarasinoside D exhibits solubility levels comparable to those of antifouling agents irgarol_1501, seanin_211, and selektope® (Table 5). These results align with recent studies on xanthone derivatives (Almeida et al. 2020), which also demonstrated moderate water solubility, indicating their suitability for incorporation into marine coatings to facilitate slow release and low bioaccumulation (Okamura et al. 2000; Chen and Lam 2017).

Given that water solubility and hydrophobicity critically influence the distribution of molecules in water, sediments, and biological tissues (Cui et al. 2014), Log K_{ow} and Log K_{oc}, of sarasinosides, AChE inhibitors, and commercial antifouling agents were calculated. As shown in Table 5, sarasinosides A1-A3 (**1-3**), D (**4**), L (**5**), M (**6**), and M2 (**7**) exhibited moderate sorption to soil and sediment, evidenced by their low Log K_{oc} values, ranging from -2.51 to -0.21 (Table 5), which are below the threshold of 3.0 (ECHA 2017). These values are lower than those observed for AChE inhibitors synoxazolidinones A (1.95) and C (1.67), and commercial antifouling agents seanine_211 (2.88) and irgarol_1501 (2.63). Conversely, econea® (**12**) and selektope® (**13**) exhibited Log K_{oc} values of 3.83 and 4.83, respectively (Table 5). This suggests that sarasinosides (**1-7**), synoxazolidinones A and C (**8-9),** irgarol_1501, and seanine_211 may not bind as well to soil and sediments when compared to econea® and selektope.

Additionally, BCF/BAF and BHL values were calculated for all compounds (**1-13**), further supporting the favorable ecotoxicological profile of sarasinosides. For instance, predicted BHL values for sarasinosides were significantly lower (between 0.0000405 and 0.00315 days in 10 g fish) compared to commercial biocides (1.48 and 211) (Table 5). Conversely, with the exception of econea® (**12**) and selektope® (**13**) BAF values of 3790 and 331 respectively, the remaining compounds (**1-11**) exhibited low predicted BAF values, ranging between 0.244 and 0.941 for sarasinosides, 1.03 and 1.45 for synoxazolidinones A and C, and 0.257 and 1.03 for irgarol_1505 and seanin_211 (Table 2). However, the calculated BCF values for sarasinosides were significantly lower (<1.0) than those of both AChE inhibitors (5.16 and 10.5) and the commercial antifoulants

(between 109 and 575) (Table 5). Since the values of >3 and 3.5 for BFA/BCF respectively are considered bioacumulative (ECHA 2017; Vilas-Boas et al. 2021), the results suggest that sarasinosides have low potential for bioaccumulation compared particularly to the commercial antifouling such as econea® and selektope®.

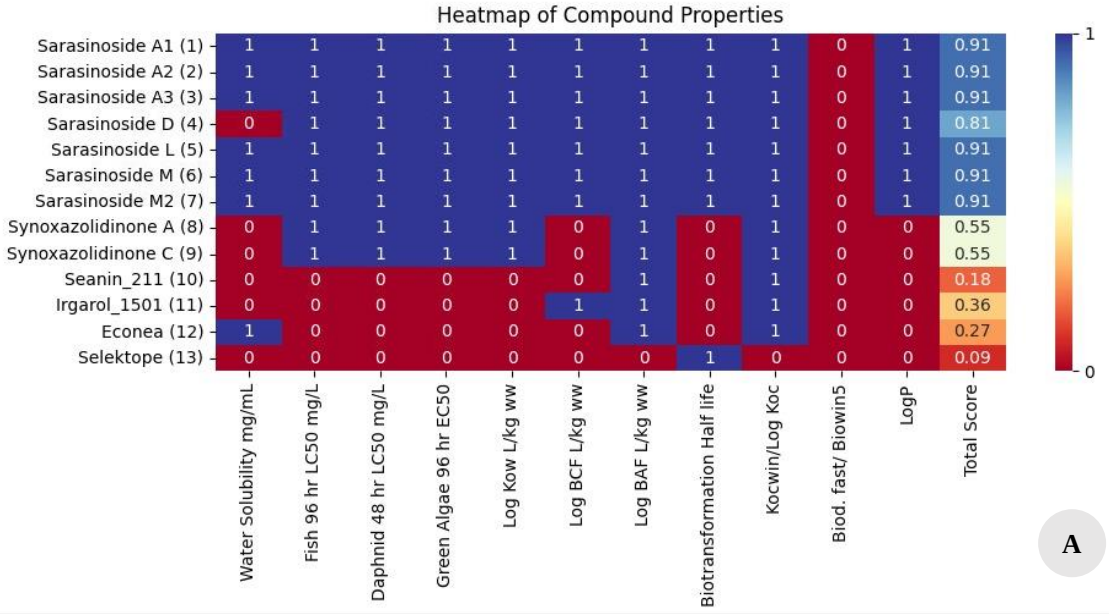


```
import matplotlib.pyplot as plt
import seaborn as sns
import numpy as np
import pandas as pd
# Create the data for the heatmap based on the provided image with corrected values for Meditominine
data_corrected_proper = np.array([
    [1, 1, 1, 1, 1, 1, 1, 1, 1,0,1,0.91], [1, 1, 1, 1, 1, 1, 1, 1, 1,0,1, 0.91], [1, 1, 1, 1, 1, 1, 1, 1, 1,0,1,0.91], [0, 1, 1, 1, 1, 1, 1, 1, 1,0,1,0.81], [1, 1, 1, 1, 1, 1, 1, 1, 1,0,1,0.91],
    [1, 1, 1, 1, 1, 1, 1, 1, 1,0,1,0.91], [1, 1, 1, 1, 1, 1, 1, 1, 1,0,1,0.91], [0, 1, 1, 1, 1, 1, 0, 1, 0, 1,0,0,0.55], [0, 1, 1, 1, 1, 1, 0, 1, 0, 1,0,0,0.55], [0, 0, 0, 0, 0, 0, 1, 0, 1,0,0,0.18],
    [0, 0, 0, 0, 0, 1, 1, 0, 1,0,0,0.36], [1, 0, 0, 0, 0, 0, 1, 0, 1,0,0,0.27], [0, 0, 0, 0, 0, 0, 0, 1, 0,0,0,0.09]])
# Create a DataFrame for the heatmap
df_corrected_proper = pd.DataFrame(data_corrected_proper, columns=[
    'Water Solubility mg/mL', 'Fish 96 hr LC50 mg/L', 'Daphnid 48 hr LC50 mg/L',
    'Green Algae 96 hr EC50', 'Log Kow L/kg ww', 'Log BCF L/kg ww',
    'Log BAF L/kg ww', 'Biotransformation Half life', 'Kocwin/Log Koc',
    'Biod. fast/ Biowin5', 'LogP', 'Total Score'
], index = [
    'Sarasinoside A1 (1)', 'Sarasinoside A2 (2)', 'Sarasinoside A3 (3)',
    'Sarasinoside D (4)', 'Sarasinoside L (5)', 'Sarasinoside M (6)',
    'Sarasinoside M2 (7)', 'Synoxazolidinone A (8)', 'Synoxazolidinone C (9)',
    'Seanin_211 (10)', 'Irgarol_1501 (11)', 'Econea (12)', 'Selektope (13)'
])
# Plot the heatmap with red for zero and blue for one
plt.figure(figsize=(12, 10))
sns.heatmap(df_corrected_proper, annot=True, cmap='RdYlBu', cbar_kws={'ticks': [0, 1]}, vmin=0, vmax=1)
plt.title('Heatmap of Compound Properties')
plt.show()
```

B

Figure 9. Heatmap of all tested compounds, showing less favorable ecotoxicological scores of 0.64 for both synoxazolidinones A and B and lower values of 0.11, 022, 0.22 and 0.44 for selektope®/. medetomidine, econea®, seanin_211 and irgarol_1501 respectively (A) and the data were generated using Phyton (https://replit.com/~) (B)

To predict the relative toxicity of sarasinosides, AChE inhibitors, and commercial antifoulants, ECOSAR™ within EPI Suite™ was used to obtain their predicted LC_{50} and EC_{50} values against fish, daphnid, and green algae (Table 5). These in silico results indicated that sarasinosides exhibited LC_{50}/EC_{50} values ranging from 10^3 to 10^8 mg/L across the tested organisms, while the commercial antifoulants ranged from 10^0 mg/L (Table 5). Specifically, calculated mean LC_{50} values of commercial antifouling compounds were 0.714 mg/L against fish and 1.737 mg/L against daphnid, whereas the mean LC_{50} value for sarasinosides were 8.17×10^7 mg/L against fish and 5.28×10^8 against daphnid, a difference spanning more than 12 orders of magnitude. This suggests that sarasinosides may exhibit more favorable toxicity profiles than commercial antifoulants. However, it is worth noting that these results are based on computational predictions and require experimental validation to confirm the actual toxicity profiles of these predicted compounds.

To asses significance of difference among sarasinosides, represented by sarasinoside A1, AChE inhibitor and the commercial antifouling, we performed Fisher's exact test (Table 7). The results indicated no significant difference in pharmacological properties values between sarasinoside A1 (**1**), with a score of 10, and the AChE inhibitors synoxazolidinones A (**8**) and C (**9**), which both had a score of 6 (Table 3) or statistically insignificant (0.1486, $p>0.05$) (Table 7). However, sarasinoside A1 demonstrated a significant difference in pharmacological values compared to the commercial antifouling agents such as seanin_211 **(9)**, irgarol_1501 (**10**), econea® (**11**), and selektope® (**13**), which exhibited much lower total scores, ranging from 2, 4, 3, and 1 (Table 3) or $p = 0.0019$, 0.0237, 0.0075 and 0.0003 respectively (Table 7). The results indicate that sarasinoside A1 exhibited similar ecotoxicological properties to the AChE inhibitors, but showed significantly different parameters compared to the commercial antifoulants, notably selektope® and seanin_211 (Table 7). The consistently higher total score (0.81-0.91) for ecotoxilogical values of the sarasinosides 1-**7** (Table 6, Figure 9) suggests they show significant beneficial values, particularly compared to the commercial antifoulants with low ecotoxicological values ranging from 0.09 to 0.36 (Table 6; Figure 9.A). A heatmap generated using Python (Figure 9.A) with its detailed syntax (Figure 9.B) further highlights the more favorable pharmacological values of sarasinosides (**1**-**7**) as eco-friendly antifouling compounds (Figure 9.A).

The sarasinosides exhibit diverse molecular structures featuring complex glycosylated steroidal frameworks characteristic of marine sponges in the genus *Melophlus* (O'Brien et al. 2023). The hydroxyl groups, glycosidic linkages, aglycone moieties, and bipolar lipid nature of sarasinosides provide unique structural features that may enhance their solubility and interaction with marine biofouling organisms. Indeed, triterpenoids with similar aglycones and glycosides have been experimentally shown to be potent antifoulants, effective against microfouling organisms, such as biofouling bacteria that form biofilms and barnacle larvae *Balanus amphitrite* (Darwin, 1854)), as well as macrofouling organisms like marine invertebrates and algae (Kalinin et al. 2012; Zhang et al. 2014; Ozupek and Cavas 2017).

The antifouling activity of triterpenoid glycosides (e.g., eryloides, sokodosides, caminosides, and sarasinoside J) has been previously correlated with antimicrobial properties (Kalinin et al. 2012). These authors argued that such antimicrobial effects are attributed to the unique bipolar lipid nature of triterpenoid glycosides, a complex and unique feature that enables their polar heads to position themselves on both the inner and outer surfaces of the lipid bilayer when penetrating host cells. However, the expected dual nature of antifouling and antibacterial activities of sarasinosides was not entirely reflected in the present study. While the extract of *M. sarasinorum* from Kawaluso Island showed antimicrobial activity against *S. aureus*, the extract of the same species from Mahumu Island did not show such activity despite containing the same collection of sarasinosides (Figures 3, 4.A-4.F). The presence of 3,5-bromotyrosine only in the extract of *M. sarasinorum* from Kawaluso Island (Figure 4.F) but not in the Mahumu Island sponge might suggest the discrepancy in antimicrobial activity. It might be speculated that 3,5-bromotyrosine in the Kawaluso sponge potentially cause additive even synergistic effects, possibly enhancing the penetration of sarasinosides into bacterial membranes, thereby leading to a more pronounced antibacterial effect of the Kawaluso extract against *S. aureus* which lacked in the extract of the Mahumu sponge (Table 1).

This hypothesis is supported by the fact that of 23 known sarasinosides, most have been frequently reported for their cytotoxic activity and less frequently for their antimicrobial activity (Kalinin et al. 2012; Ivanchina and Kalinin 2023) and 3,5-bromotyrosine is known to have antimicrobial and antifouling properties (Tintillier et al. 2020). Nonetheless, further investigations are necessary to elucidate the exact molecular mechanisms involved (Austin et al.2013; Pérez-Aguilar et al. 2023). This research aligns with ongoing efforts in antifouling discovery, as highlighted by Chen et al. (2021, 2023), who propose that effective antifouling strategies depend on synergistic interactions between the release of an antifouling agent and the prevention of biofouling. Building upon this, Chen et al. (2024b) also developed a low surface energy approach to antifouling, which facilitates the detachment of fouling organisms. The present results, where nets treated with the lowest concentration of the antifouling agent in this study exhibited the greatest antifouling performance, suggest that leveraging the properties of the substrate surface may be critical for antifouling effectiveness.

Interestingly, our molecular docking studies revealed different binding sites among sarasinosides, AChE inhibitors, and commercial antifouling agents. While AChE inhibitors (synoxazolidinones A and B) and commercial antifouling agents (irgarol_1501, selektope®, and econea®) appear to bind to the active site of AChE, specifically interacting with residues such as Trp84 and Phe331 (Luque and Muñoz-Torrero 2024), our docking models suggest sarasinosides interact with a separate putative binding site of AChE. This conclusion is supported by the lack of interactions between sarasinosides and the canonical active site residues and the

observation of unique interactions with residues such as Arg153, Tyr157, and Ser158, which are spatially distinct from the active site. These unique interactions suggest potential novel allosteric interactions between sarasinosides and AChE. These results corroborate the recent discovery of four new allosteric binding sites on AChE by Luque and Muñoz-Torrero (2024), who attempted to design synthetic compounds targeting the 20-Å-deep cavity at the active site to discover novel AChE inhibitors. By targeting known pharmacophores, such as the PAS (Peripheral Aromatic Site) and CAS (Catalytic Active Site) binding motifs of AChE, they successfully designed multitarget compounds with multiple allosteric binding sites on AChE (Luque and Muñoz-Torrero 2024). Their study supports the idea that targeting allosteric binding sites is as viable as targeting the active site of AChE, possibly leading to the discovery of new AChE inhibitors (Luque and Muñoz-Torrero 2024), and provides a foundation for future research investigating allosteric modulation of AChE by sarasinosides.

The in silico ecotoxicological evaluation of sarasinosides using EPI Suite™ revealed promising results. Most of the predicted ecotoxicological parameters (i.e., Log K_{ow}, Log K_{oc}, BHL, and Log BCF/BAF) for sarasinosides indicated a more favorable profile compared to both AChE inhibitors and commercial antifoulants. Specifically, sarasinosides exhibited significantly lower values for water solubility, Log K_{ow}, Log K_{oc}, BHL, and Log BCF/BAF, but higher LC_{50} and EC_{50} values against various aquatic organisms, than commercial antifoulants, demonstrating through computational modeling that these properties are within an acceptable range for environmentally friendly compounds. This favorable ecotoxicological profiles align with the need for safer antifouling solutions (Qiu et al. 2024) and suggest that sarasinosides could potentially mitigate environmental risks while providing effective antifouling properties. Given the current stringent regulations on antifouling agents (Georgiades et al. 2020), particularly the bans on harmful substances like TBT, the development of new agents must prioritize both efficacy and safety. Sarasinosides, with their low cytotoxicity, meet these regulatory requirements and present a viable alternative to more toxic compounds. Their compliance with environmental safety standards makes them strong candidates for approval and commercialization in the antifouling market. The initial findings of low toxicity are encouraging and warrant more extensive long-term studies to confirm their safety and environmental compatibility.

These findings have potentially significant implications for maritime industries severely impacted by biofouling. The demonstrated effectiveness of sarasinosides on treated surfaces indicates a potential shift towards more environmentally benign antifouling solutions. This research addresses the ongoing need for effective and eco-friendly antifouling agents in both the shipping and aquaculture industries (Liu et al. 2020; Gomez-Banderas 2022; Kartal and Sarıışık 2022; Zang et al. 2024). The comprehensive toxicity assessments, coupled with metabolomic, computational, and field studies, offer valuable insights into strategies for optimizing these compounds for commercial use. In contrast to current commercially available antifouling agents, such as seanin_211, irgarol_1501, selektope®, and econea®, which exhibit high toxicity levels, sarasinosides show a promising toxicity profile. By focusing on the metabolites of *M. sarasinorum*, this research suggests a methodology for evaluating their ecofriendly antifouling potential, which is a critical consideration in the broader context of sustainable marine industry practices.

Lastly, it is important to acknowledge the limitations of this study. The toxicity evaluation was conducted in-silico, which, while informative, requires validation through in vivo studies. Additionally, this study focuses on sponge powder rather than semi-pure or pure compounds, which may not fully represent the antifouling potential of sarasinosides. Future research should also address the biodegradability of sarasinosides to ensure they do not persist in marine environments. Also, the complexity of marine-derived molecules, including sarasinosides, makes their commercial production impractical despite being academically feasible in many cases, thus hindering scalability (Mehbub et al. 2024). While sponge farming and bioactive collection techniques appear feasible (Maslin et al. 2021; Carroll et al. 2022), these have not yet been applied to the production of sarasinosides from *M. sarasinorum*. Nevertheless, this study demonstrates the potential of *M. sarasinorum* powder containing sarasinosides as an eco-friendly antifouling agent. It also provides insight into the future development of more accessible antifoulants for sustainable antifouling solutions. Future research should involve detailed analysis of semi-pure or pure sarasinosides, the allosteric sites of sarasinosides on AChE and screening for molecules that bind to these sites. Furthermore, structural similarity studies using tools like SWISS similarity could identify simpler structures or the pharmacophore necessary for activity and improved pharmacological profiles.

In conclusion, this research addresses the critical need for eco-friendly antifouling agents by investigating the metabolites of the Sangihe marine sponge *M. sarasinorum* through metabolomic, computational, and field studies. The dereplicated sarasinosides A1-A3, D, L, M, and M2 showed more robust binding affinities against Acetylcholinesterase (AChE), the emerging antifouling target, and more favorable ecotoxicological parameters compared to AChE inhibitors and commercial antifoulants such as seanin_211, irgarol_1501, econea® and selektope®. While these findings highlight the promising antifouling potential of sarasinosides, further research is crucial to address long-term effects, environmental impacts, and interactions with marine organisms. Importantly, future studies should focus on evaluating the antifouling activity of pure sarasinosides, elucidating their precise mode of action through detailed analysis of allosteric sites on AChE or resolving bound complexes using protein crystallography, screening of binding molecules and sarasinosides potential mode of action linking anticancer and antifouling activities while also developing simplified analogs through structural similarity studies for improved pharmacological properties and practical application.

ACKNOWLEDGEMENTS

The authors thank the Indonesian Director General of Vocational Education, Ministry of Education, Culture, Research, and Technology, Ministry of Education, Culture, Research and Technology for financial support (No. 79/SPK/D.D4/PPK.01.APVT/III/2024). We are also grateful to Herjumes Atjin (Ucil) (Politeknik Negeri Nusa Utara, Indonesia) and Hendra Manabung for collecting the sample.

REFERENCES

Abdalla MM, Ali IAA, Khan K, Mattheos N, Murbay S, Matinlinna JP, Neelakantan P. 2021. The influence of surface roughening and polishing on microbial biofilm development on different ceramic materials. J Prosthodont 30 (5): 447-453. DOI: 10.1111/jopr.13260.

Almeida JR, Palmeira A, Campos A, Cunha I, Freitas M, Felpeto AB, Turkina MV, Vasconcelos V, Pinto M, Correia-da-Silva M, Sousa M. 2020. Structure-antifouling activity relationship and molecular targets of bio-inspired (thio) xanthones. Biomolecules 10 (8): 1126. DOI: 10.3390/biom10081126.

Arabshahi HJ, Trobec T, Foulon V, Hellio C, Frangež R, Sepčić K, Cahill P, Svenson J. 2021. Using virtual AChE homology screening to identify small molecules with the ability to inhibit marine biofouling. Front Mar Sci 8: 762287. DOI: 10.3389/fmars.2021.762287.

Aron AT, Gentry EC, McPhail KL et al. 2020. Reproducible molecular networking of untargeted mass spectrometry data using GNPS. Nat Protoc 15 (6): 1954-1991. DOI: 10.1038/s41596-020-0317-5.

Aronowitz AL, Ali SR, Glaun MDE, Amit M. 2022. Acetylcholine in carcinogenesis and targeting cholinergic receptors in oncology (Adv. Biology 9/2022). Adv Biol 6 (9): 2270091. DOI: 10.1002/adbi.202270091.

Austin P, Freeman SA, Gray CA, Gold MR, Vogl AW, Andersen RJ, Roberge M, Roskelley CD. 2013. The invasion inhibitor sarasinoside A1 reverses mesenchymal tumor transformation in an E-cadherin-independent manner. Mol Cancer Res 11 (5): 530-540. DOI: 10.1158/1541-7786.MCR-12-0385.

Ayesu EK. 2023. Does shipping cause environmental emissions? Evidence from African countries. Transp Res Interdiscip Persp 21: 100873. DOI: 10.1016/j.trip.2023.100873.

Balansa W, Riyanti, Manurung UN, Tomasoa AM, Hanif N, Rieuwpassa FJ, Schäberle TF. 2024. Sponge-based ecofriendly antifouling: Field study on nets, molecular docking with agelasine alkaloids. Trop J Nat Prod Res 8 (1): 5913-5924. DOI: 10.26538/tjnpr/v8i1.29.

Balansa W. 2014. Discovery of novel, potent and selective glycine receptor modulators from Southern Australian sponges. [Dissertation]. Institute for Molecular Bioscience, The University of Queensland. DOI: 10.14264/uql.2016.29.

Bannister J, Sievers M, Bush F, Bloecher N. 2019. Biofouling in marine aquaculture: A review of recent research and developments. Biofouling 35 (6): 631-648. DOI: 10.1080/08927014.2019.1640214.

Bhal SK. 2007. LogP—Making Sense of the Value. Advanced Chemistry Development. Toronto, ON. Canada.

Byers JE, Blaze JA, Dodd AC, Hall HL, Gribben PE. 2023. Exotic asphyxiation: Interactions between invasive species and hypoxia. Biol Rev Camb Philos Soc 98 (1): 150-167. DOI: 10.1111/brv.12900.

Card ML, Gomez-Alvarez V, Lee W-H, Lynch DG, Orentas NS, Lee MT, Wong EM, Boethling RS. 2017. History of EPI Suite™ and future perspectives on chemical property estimation in US toxic substances control act new chemical risk assessments. Environ Sci Process Impacts 19 (3): 203-212. DOI: 10.1039/c7em00064b.

Carroll AR, Copp BR, Davis RA, Keyzers RA, Prinsep MR. 2022. Marine natural products. Nat Prod Rep 39 (6): 1122-1171. DOI: 10.1039/D1NP00076D.

Chen J, Bai W, Jian R, Lin Y, Zheng X, Wei F, Lin Q, Lin F, Xu Y. 2024a. Molecular structure design of polybenzoxazines with low surface energy and low modulus for marine antifouling application. Prog Org Coat 187: 108165. DOI: 10.1016/j.porgcoat.2023.108165.

Chen J, Jian R, Yang K, Bai W, Huang C, Lin Y, Zheng B, Wei F, Lin Q, Xu Y. 2021. Urushiol-based benzoxazine copper polymer with low surface energy, strong substrate adhesion and antibacterial for marine antifouling application. J Clean Prod 318: 128527. DOI: 10.1016/j.jclepro.2021.128527.

Chen J, Zhao J, Lin F, Zheng X, Jian R, Lin Y, Wei F, Lin Q, Bai W, Xu Y. 2023. Polymerized tung oil toughened urushiol-based benzoxazine copper polymer coatings with excellent antifouling performances. Prog Org Coat 177: 107411. DOI: 10.1016/j.porgcoat.2023.107411.

Chen J, Zheng X, Jian R, Bai W, Zheng G, Xie Z, Lin Q, Lin F, Xu Y. 2024b. In situ reduction of silver nanoparticles/urushiol-based polybenzoxazine composite coatings with enhanced antimicrobial and antifouling performances. Polymers 16 (8): 1167. DOI: 10.3390/polym16081167.

Chen L, Lam JCW. 2017. SeaNine 211 as antifouling biocide: A coastal pollutant of emerging concern. J Environ Sci 61: 68-79. DOI: 10.1016/j.jes.2017.03.040.

Costanzo LG, Marletta G, Alongi G. 2021. Non-indigenous macroalgal species in coralligenous habitats of the marine protected area Isole Ciclopi (Sicily, Italy). Ital Bot 11: 31-44. DOI: 10.3897/italianbotanist.11.60474.

Cui YT, Teo SLM, Leong W, Chai CLL. 2014. Searching for "environmentally-benign" antifouling biocides. Intl J Mol Sci 15 (6): 9255-9284. DOI: 10.3390/ijms15069255.

Cuthbert RN, Pattison Z, Taylor NG et al. 2021. Global economic costs of aquatic invasive alien species. Sci Total Environ 775: 145238. DOI: 10.1016/j.scitotenv.2021.145238.

Dai HF, Edrada RA, Ebel R, Nimtz M, Wray V, Proksch P. 2005. Norlanostane triterpenoidal saponins from the marine Sponge *Melophlus sarassinorum*. J Nat Prod 68: 1231-1237. DOI: 10.1021/np050152d.

Dobretsov S, Rittschof D. 2023. "Omics" Techniques used in marine biofouling studies. Intl J Mol Sci 24 (13): 10518. DOI: 10.3390/ijms241310518.

ECHA [Environment and Climate Change Canada]. 2017. Guidance on information requirements and chemical safety assessment. Environment and Climate Change, Canada.

ECHA [Environment and Climate Change Canada]. 2021. Toxic substances list: schedule 1 (Tech.). Retrieved from https://www.canada.ca/en/environment-climate-change/services/canadian-environmental-protection-act-registry/substances-list/toxic/schedule-1.html.

Farkas A, Degiuli N, Martić I, Vujanović M. 2021. Greenhouse gas emissions reduction potential by using antifouling coatings in a maritime transport industry. J Clean Prod 295: 126428. DOI: 10.1016/j.jclepro.2021.126428.

Ferreira Montenegro P, Pham GN, Abdoul-Latif FM, Taffin-de-Givenchy E, Mehiri M. 2024. Marine bromotyrosine derivatives in spotlight: Bringing discoveries and biological significance. Mar Drugs 22 (3): 132. DOI: 10.3390/md22030132.

Gaudêncio SP, Pereira F. 2022. Predicting antifouling activity and acetylcholinesterase inhibition of marine-derived compounds using a computer-aided drug design approach. Mar Drugs 20 (2): 129. DOI: 10.3390/md20020129.

Georgiades E, Kluza D, Bates T, Lubarsky K, Brunton J, Growcott A, Smith T, McDonald S, Gould B, Parker N, Bell A. 2020. Regulating vessel biofouling to support New Zealand's marine biosecurity system-a blue print for evidence-based decision making. Front Mar Sci 7: 390. DOI: 10.3389/fmars.2020.00390.

Georgiades E, Scianni C, Davidson I, Tamburri MN, First MR, Ruiz G, Ellard K, Deveney M, Kluza D. 2021. The role of vessel biofouling in the translocation of marine pathogens: Management considerations and challenges. Front Mar Sci 8: 660125. DOI: 10.3389/fmars.2021.660125.

Gomez-Banderas J. 2022. Marine natural products: A promising source of environmentally friendly antifouling agents for the maritime industries. Front Mar Sci 9: 858757. DOI: 10.3389/fmars.2022.858757.

Hadžić N, Gatin I, Uroić T, Ložar V. 2022. Biofouling dynamic and its impact on ship powering and dry-docking. Ocean Eng 245: 110522. DOI: 10.1016/j.oceaneng.2022.110522.

Hodson SL, Lewis TE, Burkea CM. 1997. Biofouling of fish-cage netting: Efficacy and problems of in situ cleaning. Aquaculture 152 (1-4): 77-90. DOI: 10.1016/s0044-8486(97)00007-0.

Hooper JNA, Van Soest RWM. 2002. Systema Porifera: A Guide to The Supraspecific Classification of The Phylum Sponges. Kluwer Academic/Plenum Publishers, New York.

Ivanchina NV, Kalinin VI. 2023. Triterpene and steroid glycosides from marine sponges (Porifera, Demospongiae): Structures, taxonomical distribution, biological activities. Molecules 28 (6): 2503. DOI: 10.3390/molecules28062503.

James GA, Boegli L, Hancock J, Bowersock L, Parker A, Kinney BM. 2019. Bacterial adhesion and biofilm formation on textured breast implant shell materials. Aesthetic Plast Surg 43 (2): 490-497. DOI: 10.1007/s00266-018-1234-7.

Johnson G, Moore SW. 2006. The peripheral anionic site of acetylcholinesterase: Structure, functions and potential role in rational drug design. Curr Pharm Des 12 (2): 217-225. DOI: 10.2174/138161206775193127.

Kalinin VI, Ivanchina NV, Krasokhin VB, Makarieva TN, Stonik VA. 2012. Glycosides from marine sponges (porifera, Demospongiae): Structures, taxonomical distribution, biological activities and biological roles. Mar Drugs 10 (8): 1671-1710. DOI: 10.3390/md10081671.

Kartal GE, Sarıışık AM. 2022. Providing antifouling properties to fishing nets with encapsulated Econea. J Indust Text 51: 7569S-7586S. DOI: 10.1177/1528083720920568.

Kobayashi M, Okamoto Y, Kitagawa I. 1991. Marine natural products. XXVIII. The structures of sarasinosides A1, A2, A3, B1, B2, B3, C1, C2, and C3, nine new norlanostane-triterpenoidal oligoglycosides from the Palauan marine sponge *Asteropus sarasinosum*. Chem Pharm Bull 39 (11): 2867-2877.

Kobayashi Y. 2021. Analysis of The Environmental Parameters for Risk Assessment of Pesticides by Machine Learning Approach. [Dissertation]. University of Tsukuba, Japan.

Lee D-H, Eom H-J, Kim M, Jung J-H, Rhee J-S. 2017. Non-target effects of antifouling agents on mortality, hatching success, and acetylcholinesterase activity in the brine shrimp *Artemia salina*. Toxicol Environ Health Sci 9: 237-243. DOI: 10.1007/s13530-017-0326-0.

Liu H, Yang W, Zhao W, Zhang J, Cai M, Pei X, Zhou F. 2020. Natural product inspired environmentally friendly strategy based on dopamine chemistry toward sustainable marine antifouling. ACS Omega 5 (34): 21524-21530. DOI: 10.1021/acsomega.0c02114.

Luque FJ, Muñoz-Torrero D. 2024. Acetylcholinesterase: A versatile template to coin potent modulators of multiple therapeutic targets. Acc Chem Res 57 (4): 450-467. DOI: 10.1021/acs.accounts.3c00617.

Mackay D, Fraser A. 2000. Bioaccumulation of persistent organic chemicals: Mechanisms and models. Environ Pollut 110 (3): 375-391. DOI: 10.1016/S0269-7491(00)00162-7.

Marcelo F, Dias C, Martins A, Madeira PJ, Jorge T, Florêncio MH, Cañada FJ, Cabrita EJ, Jiménez-Barbero J, Rauter AP. 2013. Molecular recognition of rosmarinic acid from *Salvia sclareoides* extracts by acetylcholinesterase: A new binding site detected by NMR spectroscopy. Chemistry 19 (21): 6641-6649. DOI: 10.1002/chem.201203966.

Marucci G, Buccioni M, Ben DD, Lambertucci C, Volpini R, Amenta F. 2021. Efficacy of acetylcholinesterase inhibitors in Alzheimer's disease. Neuropharmacology 190: 108352. DOI: 10.1016/j.neuropharm.2020.108352.

Maslin M, Gaertner-Mazouni N, Debitus C, Joy N, Ho R. 2021. Marine sponge aquaculture towards drug development: An ongoing history of technical, ecological, chemical considerations and challenges. Aquac Rep 21: 100813. DOI: 10.1016/j.aqrep.2021.100813.

Mehbub MF, Yang Q, Cheng Y, Franco CMM, Zhang W. 2024. Marine sponge-derived natural products: Trends and opportunities for the decade of 2011-2020. Front Mar Sci 11: 1462825. DOI: 10.3389/fmars.2024.1462825.

Nogueira RD, Silva CB, Lepri CP, Palma-Dibb RG, Geraldo-Martins VR. 2017. Evaluation of surface roughness and bacterial adhesion on tooth enamel irradiated with high intensity lasers. Braz Dent J 28 (1): 24-29. DOI: 10.1590/0103-6440201701190.

Nong X-H, Wang Y-F, Zhang X-Y, Zhou M-P, Xu X-Y, Qi S-H. 2014. Territrem and butyrolactone derivatives from a marine-derived fungus *Aspergillus terreus*. Mar Drugs 12 (12): 6113-6124. DOI: 10.3390/md12126113.

O'Brien S, Lacret R, Reddy MM, Jennings LK, Sánchez P, Reyes F, Mungkaje A, Calabro K, Thomas OP. 2023. Additional sarasinosides from the marine sponge *Melophlus sarasinorum* collected from the Bismarck Sea. J Nat Prod 86 (12): 2730-2738. DOI: 10.1021/acs.jnatprod.3c01045.

Okamura H, Aoyama I, Liu D, Maguire RJ, Pacepavicius GJ, Lau YL. 2000. Fate and ecotoxicity of the new antifouling compound irgarol 1051 in the aquatic environment. Water Res 34 (14): 3523-3530. DOI: 10.1016/s0043-1354(00)00095-6.

Olick D. 2023. Shipping industry could lose S10 billiong a year battling climate change by 2050. CNBC. https://www.cnbc.com/2023/10/30/climate-change-to-cost-shipping-industry-10-billion-a-year-by-2050.html.

Ozupek NM, Cavas L. 2017. Triterpene glycosides associated antifouling activity from *Holothuria tubulosa* and *H. polii*. Reg Stud Mar Sci 13: 32-41. DOI: 10.1016/j.rsma.2017.04.003.

Pérez-Aguilar B, Marquardt JU, Muñoz-Delgado E, López-Durán RM, Gutiérrez-Ruiz MC, Gomez-Quiroz LE, Gómez-Olivares JL. 2023. Changes in the Acetylcholinesterase enzymatic activity in tumor development and progression. Cancers 15 (18): 4629. DOI: 10.3390/cancers15184629.

Pinteus S, Lemos MFL, Alves C, Silva J, Pedrosa R. 2021. The marine invasive seaweeds *Asparagopsis armata* and *Sargassum muticum* as targets for greener antifouling solutions. Sci Total Environ 750: 141372. DOI: 10.1016/j.scitotenv.2020.141372.

Puentes C, Carreño K, Santos-Acevedo M, Gómez-León J, García M, Pérez M, Stupak M, Blustein G. 2014. Antifouling paints based on extracts of marine organisms from the Colombian Caribbean. Cienc Tecnol Buq 8 (15): 75-90. DOI: 10.25043/19098642.105.

Qian P-Y, Li Z, Xu Y, Li Y, Fusetani N. 2015. Mini-review: Marine natural products and their synthetic analogs as antifouling compounds: 2009-2014. Biofouling 31 (1): 101-122. DOI: 10.1080/08927014.2014.997226.

Qiu Q, Gu Y, Ren Y, Ding H, Hu C, Wu D, Mou J, Wu Z, Dai D. 2024. Research progress on eco-friendly natural antifouling agents and their antifouling mechanisms. Chem Eng J 495: 153638. DOI: 10.1016/j.cej.2024.153638.

Quémener M, Kikionis S, Fauchon M, Toueix Y, Aulanier F, Makris AM, Roussis V, Ioannou E, Hellio C. 2021. Antifouling activity of halogenated compounds derived from the red alga *Sphaerococcus coronopifolius*: Potential for the development of environmentally friendly solutions. Mar Drugs 20 (1): 32. DOI: 10.3390/md20010032.

Rieuwpassa FJ, Tomasoa AM, Palawe JFP, Rieuwpassa F, Mege RA, Balansa W. 2023. A new and practical method for measuring sponge. Jurnal Ilmiah Platax 11: 322-332. DOI: 10.35800/jip.v10i2.47882.

Riyanti, Balansa W, Liu Y et al. 2020b. Selection of sponge-associated bacteria with high potential for the production of antibacterial compounds. Sci Rep 10: 19614. DOI: 10.1038/s41598-020-76256-2.

Riyanti, Marner M, Hartwig C, Patras MA, Wodi SIM, Rieuwpassa FJ, Ijong FG, Balansa W, Schäberle TF. 2020a. Sustainable low-volume analysis of environmental samples by semi-automated prioritization of extracts for natural product research (SeaPEPR). Mar Drugs 18 (12): 649. DOI: 10.3390/md18120649.

Roca C, Requena C, Sebastián-Pérez V, Malhotra S, Radoux C, Pérez C, Martinez A, Páez JA, Blundell TL, Campillo NE. 2018. Identification of new allosteric sites and modulators of AChE through computational and experimental tools. J Enzyme Inhib Med Chem 33 (1): 1034-1047. DOI: 10.1080/14756366.2018.1476502.

Roney M, Mohd Aluwi MFF. 2024. The importance of in-silico studies in drug discovery. Intell Pharm 2 (4): 578-579. DOI: 10.1016/j.ipha.2024.01.010.

Ross JG, Graham BJ, Pitt KA. 2024. Predator-free New Zealand 2050: Techniques for improving ground-based control and monitoring of the Brushtail Possum. Proc Vertebr Pest Conf 31: 1-5.

Selim MS, Shenashen MA, El-Safty SA, Higazy SA, Selim MM, Isago H, Elmarakbi A. 2017. Recent progress in marine foul-release polymeric nanocomposite coatings. Prog Mater Sci 87: 1-32. DOI: 10.1016/j.pmatsci.2017.02.001.

Song S, Muscat-Fenech CDM, Demirel YK. 2021. Economic and environmental impacts of antifouling coatings used on the fishing boats in Turkey. In: 2nd International Conference on Ship and Marine Technology. https://www.gmoshipmar.org/GMOSHIPMAR2021/.

Stowe SD, Richards JJ, Tucker AT, Thompson R, Melander C, Cavanagh J. 2011. Anti-biofilm compounds derived from marine sponges. Mar Drugs 9 (10): 2010-2035. DOI: 10.3390/md9102010.

Sumner LW, Amberg A, Barrett D et al. 2007. Proposed minimum reporting standards for chemical analysis: Chemical Analysis Working Group (CAWG) Metabolomics Standards Initiative (MSI). Metabolomics 3 (3): 211-221. DOI: 10.1007/s11306-007-0082-2.

Sussman JL, Harel M, Frolow F, Oefner C, Goldman A, Toker L, Silman I. 1991. Atomic structure of acetylcholinesterase from *Torpedo californica*: A prototypic acetylcholine-binding protein. Science 253 (5022): 872-879. DOI: 10.1126/science.1678899.

Tadesse M, Svenson J, Sepčić K, Trembleau L, Engqvist M, Andersen JH, Jaspars M, Stensvåg K, Haug T. 2014. Isolation and synthesis of pulmonarins A and B, acetylcholinesterase inhibitors from the colonial ascidian *Synoicum pulmonaria*. J Nat Prod 77 (2): 364-369. DOI: 10.1021/np401002s.

Tintillier F, Moriou C, Petek S, Fauchon M, Hellio C, Saulnier D, Ekins M, Hooper JNA, Al-Mourabit A, Debitus C. 2020. Quorum sensing inhibitory and antifouling activities of new Bromotyrosine metabolites from the Polynesian sponge *Pseudoceratina* n. sp. Mar Drugs 18 (5): 272. DOI: 10.3390/md18050272.

Van Gestel CA, Otermann K, Canton JH. 1985. Relation between water solubility, cctanol/water partition coefficients, and bioconcentration of organic chemicals in fish: A review. Regul Toxicol Pharmacol 5 (4): 422-431. DOI: 10.1016/0273-2300(85)90007-8.

Vilas-Boas C, Neves AR, Carvalhal F et al. 2021. Multidimensional characterization of a new antifouling xanthone: Structure-activity relationship, environmental compatibility, and immobilization in marine coatings. Ecotoxicol Environ Saf 228: 112970. DOI: 10.1016/j.ecoenv.2021.112970.

Vilas-Boas C, Silva ER, Resende D, Pereira B, Sousa G, Pinto M, Almeida JR, Correia-da-Silva M, Sousa M. 2023. 3,4-Dioxygenated xanthones as antifouling additives for marine coatings: In silico studies, seawater solubility, degradability, leaching, and antifouling performance. Environ Sci Pollut Res Intl 30 (26): 68987-68997. DOI: 10.1007/s11356-023-26899-1.

Wassmann T, Kreis S, Behr M, Buergers R. 2017. The influence of surface texture and wettability on initial bacterial adhesion on titanium and zirconium oxide dental implants. Intl J Implant Dent 3 (1): 32. DOI: 10.1186/s40729-017-0093-3.

Xing R, Lyngstadaas SP, Ellingsen JE, Taxt-Lamolle S, Haugen HJ. 2015. The influence of surface nano roughness, texture and chemistry of TiZr implant abutment on oral biofilm accumulation. Clin Oral Implants Res 26 (6): 649-656. DOI: 10.1111/clr.12354.

Yao W-L, Lin JCY, Salamanca E, Pan Y-H, Tsai P-Y, Leu S-J, Yang K-C, Huang H-M, Huang H-Y, Chang W-J. 2020. YSGG laser performance improves biological response on titanium surfaces. Materials 13 (3): 756. DOI: 10.3390/ma13030756.

Yousef ANAA. 2023. Examining the effects of biofouling on ships and how it contributes to the introduction of non-native species in newly discovered coastal areas in biofouling on ship hulls and its ecological ramification. SSRN Electronic J 2024: 1-26. DOI: 10.2139/ssrn.4666557.

Yu P, Wang C, Zhou J, Jiang L, Xue J, Li W. 2016. Influence of surface properties on adhesion forces and attachment of *Streptococcus mutans* to zirconia in vitro. Biomed Res Intl 2016: 8901253. DOI: 10.1155/2016/8901253.

Zang X, Ni Y, Wang Q, Cheng Y, Huang J, Cao X, Carmalt CJ, Lai Y, Kim DH, Liu Y, Lin Z. 2024. Non-toxic evolution: Advances in multifunctional antifouling coatings. Mater Today 75: 210-243. DOI: 10.1016/j.mattod.2024.03.018.

Zhang J, Liang Y, Wang K-L, Liao X-J, Deng Z, Xu S-H. 2014. Antifouling steroids from the South China Sea gorgonian coral *Subergorgia suberosa*. Steroids 79: 1-6. DOI: 10.1016/j.steroids.2013.10.007.

Zheng S, Bawazir M, Dhall A, Kim H-E, He L, Heo J, Hwang G. 2021. Implication of surface properties, bacterial motility, and hydrodynamic conditions on bacterial surface sensing and their initial adhesion. Front Bioeng Biotechnol 9: 634722. DOI: 10.3389/fbioe.2021.643722.